The Journal of Experimental Biology 202, 1603–1623 (1999)
Printed in Great Britain © The Company of Biologists Limited 1999
JEB1964

MANY-LEGGED MANEUVERABILITY: DYNAMICS OF TURNING IN HEXAPODS

DEVIN L. JINDRICH AND ROBERT J. FULL*
Department of Integrative Biology, University of California at Berkeley, Berkeley, CA 94720, USA
*Author for correspondence (e-mail: rjfull@socrates.berkeley.edu)

Accepted 12 March; published on WWW 20 May 1999

Summary

Remarkable similarities in the vertical plane of forward motion exist among diverse legged runners. The effect of differences in posture may be reflected instead in maneuverability occurring in the horizontal plane. The maneuver we selected was turning during rapid running by the cockroach *Blaberus discoidalis*, a sprawled-postured arthropod. Executing a turn successfully involves at least two requirements. The animal's mean heading (the direction of the mean velocity vector of the center of mass) must be deflected, and the animal's body must rotate to keep the body axis aligned with the heading. We used two-dimensional kinematics to estimate net forces and rotational torques, and a photoelastic technique to estimate single-leg ground-reaction forces during turning. Stride frequencies and duty factors did not differ among legs during turning. The inside legs ended their steps closer to the body than during straight-ahead running, suggesting that they contributed to turning the body. However, the inside legs did not contribute forces or torques to turning the body, but actively pushed against the turn. Legs farther from the center of rotation on the outside of the turn contributed the majority of force and torque impulse which caused the body to turn. The dynamics of turning could not be predicted from kinematic measurements alone. To interpret the single-leg forces observed during turning, we have developed a general model that relates leg force production and leg position to turning performance. The model predicts that all legs could turn the body. Front legs can contribute most effectively to turning by producing forces nearly perpendicular to the heading, whereas middle and hind legs must produce additional force parallel to the heading. The force production necessary to turn required only minor alterations in the force hexapods generate during dynamically stable, straight-ahead locomotion. A consideration of maneuverability in the horizontal plane revealed that a sprawled-postured, hexapodal body design may provide exceptional performance with simplified control.

Key words: locomotion, control, curve-walking, mechanics, insect, arthropod, cockroach, *Blaberus discoidalis*.

Introduction

Sprawled-postured arthropods can be both highly statically stable and remarkably maneuverable. The common perception of a reciprocal relationship between stability and maneuverability is false for animals such as rapidly running cockroaches and crabs. Although many-legged, sprawled-postured arthropods can be highly statically stable (i.e. the center of mass lies within at least a tripod of support; Alexander, 1971), this static stability does not preclude dynamics from influencing locomotion (Ting et al., 1994). Force, velocity and inertia are important for maintaining stable motion, particularly at high speeds. For example, ignoring the dynamics of many-legged, sprawled-postured arthropods would have prevented the discovery that diverse legged animals can all be modeled by a simple spring-mass system (Blickhan and Full, 1987; Full, 1989; Full and Tu, 1990, 1991). Bipedal runners and hoppers as well as four-, six- and eight-legged trotters maintain a stable, re-entrant path of their center of mass in the vertical plane of forward motion from step to step in a very similar way (Alexander, 1990; Blickhan, 1989; Blickhan and Full, 1993; Cavagna et al., 1977; Farley et al., 1993; Full and Farley, 1999; McMahon and Cheng, 1990). Diverse morphologies can all employ bouncing dynamics during straight-ahead running.

The generality of spring-mass dynamics naturally raises the question of when leg morphology influences locomotion. The advantages and disadvantages of increased leg number and sprawled posture during running remain speculative. However, we do know that spring-mass dynamics is not attained by using all the legs in a similar manner. During constant average-speed, straight-ahead running, cockroaches operate like a spring-mass system in which three legs sum to operate as one leg of a biped or two legs of a quadruped. Each leg of the tripod (a front leg and hind leg on one side and a middle leg on the other) functions differently (Full et al., 1991). The front (prothoracic) pair of legs only decelerates the insect during the stance phase, while at the same time the hind (metathoracic) pair of legs only accelerates the animal forward. The middle (mesothoracic) pair of legs works much like human legs. The middle pair first

decelerates and then accelerates the body during a step. Ground-reaction forces tend to align along the axis of each leg, minimizing joint torque (Full et al., 1991).

We propose that differential leg function and morphology also enable statically stable, many-legged animals to be remarkably maneuverable. The present study examines turning, a maneuver that takes place primarily in the horizontal plane. Two principal turning strategies have been proposed for insects: increasing step frequency (Graham, 1972; Zolotov et al., 1975) or step length (Franklin et al., 1981; Frantsevich and Mokrushov, 1980; Graham, 1972; Jander, 1985; Strauß and Heisenberg, 1990; Zollikofer, 1994; Zolotov et al., 1975) of legs on one side of the body relative to the other. At the extreme of changes in step length, some insects may fix one leg in place (Frantsevich and Mokrushov, 1980; Zolotov et al., 1975) and pivot about it, or move the legs on one side of the body backwards (Franklin et al., 1981; Frantsevich and Mokrushov, 1980; Zolotov et al., 1975). Additional changes in step geometry, such as alterations in the functional length of the legs, have also been observed (Franklin et al., 1981).

Changes in stride frequency or stride length must act to turn the body by causing translational and rotational accelerations that result in the alterations in heading (the direction of the velocity vector of the center of mass) and body orientation observed during a turn. Legs may act in different ways to produce these accelerations during turning (Hughes, 1989), analogous to the differential leg function observed during straight-ahead running. Camhi and Levy (1988) addressed the possibility that motions of some legs during turning may reflect active contributions to turning and that motions of other legs may be due to motion of the body relative to the position of the foot on the substratum. This possibility underscores the fact that kinematic measurements alone may not reflect the different contributions of individual legs to moving the body, as has been emphasized in several studies of maneuverability in arthropods (Camhi and Levy, 1988; Cruse and Silva Saavedra, 1996; Domenici et al., 1998; Hughes, 1989; Land, 1972). Recent research (Domenici et al., 1998) has made progress towards separating leg movements due to active contributions by legs, or sets of legs, to turning from movements due to body motion in unrestrained, intact animals. We contend that it is necessary to add a consideration of kinetics (force and inertia) to kinematic measurements to understand the potential benefits of the turning strategies used by many-legged animals. Understanding the full movement dynamics also allows us to generate hypotheses about how leg and body morphology and function affect potential turning performance.

We take the next step in elucidating the mechanisms of maneuverability by measuring the full dynamics of turning. Executing a successful turn involves at least two requirements. First, the animal's mean heading must change from an initial direction during straight-ahead running to a new direction (Fig. 1A). This angle of deflection of the center of mass (COM) trajectory (θ_d) depends on the magnitude of the perpendicular force impulse (F_p, the force perpendicular to the initial heading, integrated over the step period) relative to the forward momentum of the COM (the product of body mass and forward velocity).

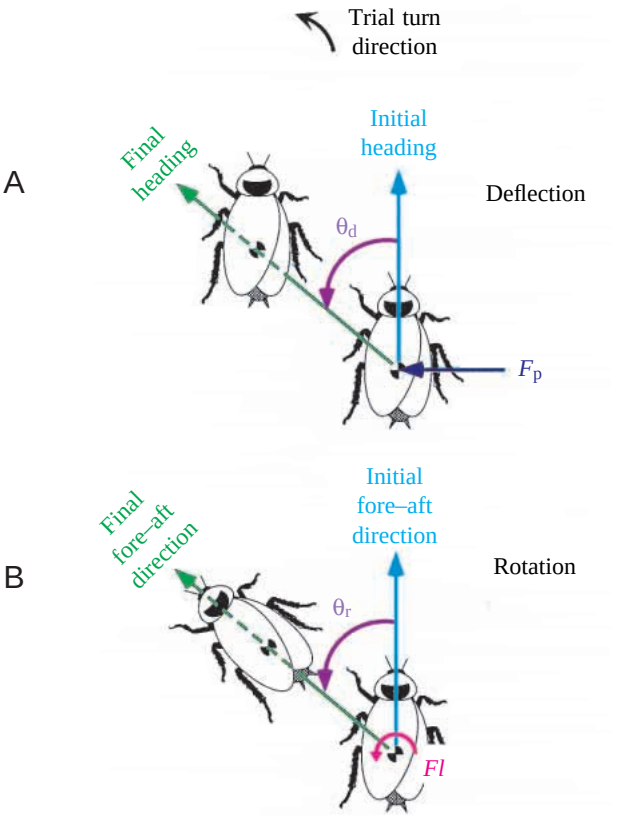

Fig. 1. Turning hypotheses. (A) To turn, the animal must deflect the direction of the velocity vector of its center of mass (the heading) from an initial heading to a final heading. This requires a force perpendicular to the heading, F_p. The magnitude of this deflection is θ_d. (B) The animal must also rotate its body by θ_r to maintain the fore–aft axis aligned with the heading axis at the end of the turn. This requires a torque, Fl, where F is the resultant horizontal force and l is the moment arm (see Fig. 2).

A second requirement for a successful turn involves rotating the fore–aft axis (represented by a line through the COM and the head) so that it aligns with the heading (Fig. 1B). To minimize the degree of misalignment between deflection and body rotation, the torque impulse (net torque integrated over the step period) relative to the inertia of the body about the yaw axis must cause a rotation (θ_r) equal to the heading deflection.

The specific objective of the present study was to determine the forces and torques necessary to produce a turn and the legs responsible for force and torque production. We chose to study turning in the death-head cockroach *Blaberus discoidalis* because of the complete, three-dimensional, dynamic data already available for straight-ahead running (Blickhan and Full, 1987; Full and Ahn, 1995; Full et al., 1991, 1998; Full and Tu, 1990, 1991; Kram et al., 1997). From the two-dimensional kinematics of turning, we estimated the net perpendicular forces and rotational torques on the COM. Since many-legged animals, such as cockroaches, typically have

more than one leg on the substratum at one time, the force and torque contributions of individual legs to the net force and torque on the COM are indeterminate. By estimating single-leg ground-reaction forces using a photoelastic technique (Full et al., 1995), we determined which legs were responsible for the force and torque production necessary to turn the body. We interpreted the data using a simple, general model which relates leg function (i.e. force production) and morphology (i.e. leg position) to turning performance.

Materials and methods

Animals

We used the death-head cockroach *Blaberus discoidalis* (Serville), with a mass of 4.6±0.26 g (mean ± S.D., N=6). Cockroaches were housed in plastic containers and fed dog food and water *ad libitum.*

Apparatus

We used a photoelastic technique to measure single-leg forces from freely moving cockroaches (Full et al., 1995). The light source for all trials was a projector (Dukane, model 653, with a 360 W bulb). We constructed two large gelatin plates by gluing pieces of glass 0.32 cm thick onto a 40.5 cm×40.5 cm square glass bottom to form a square well 0.32 cm deep. One plate had a 28.6 cm×28.6 cm square well, and the second plate had a 24.5 cm×24.5 cm square well. A linear polarizer (a sheet of Polaroid HN38S) was attached to the bottom of the plates so that the polarizing axis was parallel to one side of the well. A lens-mounted polarizer (Edmund Scientific photo mount polarizing filter) served as an upper filter. We constructed an acrylic track with a 15.5 cm deep × 10 cm wide × 71 cm long runway leading to a 15.5 cm deep × 21 cm wide × 25.4 cm long open area. The gelatin plates formed the floor of the open area and were held by the track 22.5 cm above the ground and 2.54 cm above the projector. Fiber-optic lights provided epiluminescence. Epiluminescence did not affect the appearance of the gelatin or the stress-induced light patterns.

The track was constructed so that the cockroaches emerged from a relatively narrow chute into the open area and onto the gelatin surface, where they were confronted by a curved or slanted cardboard wall in their direction of motion. The cockroaches had to turn or stop to avoid hitting the wall. Towards the rear of the open area was a darkened refuge where the cockroaches could retreat after turning.

We prepared the gelatin slabs in the same manner as described by Full et al. (1995). During video-taping, we moistened and cleaned the gelatin by wiping it with lint-free tissue and a mild soap solution. After wiping the gelatin, we allowed it to dry until the gelatin was moist enough that the cockroaches neither slipped on the gelatin nor stuck to it.

Video recording

We video-taped trials from above at 500 frames s^{-1} using a high-speed camera (Kodak Ektapro 1000 with an image intensifier or a Redlake Motionscope). The camera was positioned above the track to make its field of view approximately 12 cm×10 cm. A field of view that is as small as possible maximizes the resolution of the video for the most accurate gelatin force recordings. However, the field of view must also be large enough to allow multiple steps within the field of view. Video-taped segments were then transferred to computer files using a frame-grabbing board (Neotech Image Grabber, NUBus) and software (program implemented using Ultimage Concept V.i., Graftek, France, package for LabVIEW 2.2.1, National Instruments).

Experimental protocol

Cockroaches were not trained prior to testing. The animals were stimulated to run down the track by lightly touching their cerci. All trials were video-taped, but only trials in which the cockroach turned in the field of view of the camera, without slipping or sticking to the gelatin, were considered for analysis. Of these, we only selected trials for analysis in which the legs of the animal and the optical patterns were minimally obscured by the body. To qualify as a turn produced during running, the fore–aft axis angle had to change by more than 20 ° and the initial velocity had to be greater than 15 cm s^{-1}.

The probability of a successful trial was approximately 1 %. Many factors prevented analysis of trials. Cockroaches preferred to stay close to the walls while running (Camhi and Johnson, 1999) and often decelerated and stopped. Their legs and body frequently hit the wall. Moreover, the walls distorted or obscured the optical patterns produced by their tarsi.

We accepted eleven trials from six animals. From these trials, we analyzed the force developed by 41 steps (i.e. tripods), consisting of 114 individual leg steps. In total, 3560 individual leg force patterns from 1584 images were digitized. Seven trials consisted of at least two strides (four steps) and were used for kinematic analysis.

Kinematics

We used a motion-analysis system (Peak Performance Technology, Peak 5 and Motus) to determine the two-dimensional kinematics of turning. We digitized the head, the midpoint on the axis between the head and the end of the abdomen or ‘tail’ and tail points over the course of the trial. These data were filtered using a fourth-order Butterworth low-pass filter with zero phase shift (LabVIEW 4.0.2 program, National Instruments) at a cut-off frequency of 25 Hz. The fore–aft axis angle (the angle between the fore–aft axis and the global x-axis, defined to be the constant horizontal axis of the video image; Fig. 2A) was calculated from the head and tail points. If the head or tail point of the animal moved outside the field of view, the fore–aft axis angle was calculated from the midpoint and the head or tail point in the field of view. We estimated the position of the COM as a point 54 % of the body length along the fore–aft axis from the head (Kram et al., 1997).

We digitized tarsal or ‘foot’ touchdown positions by approximating the position of the center of the optical pattern

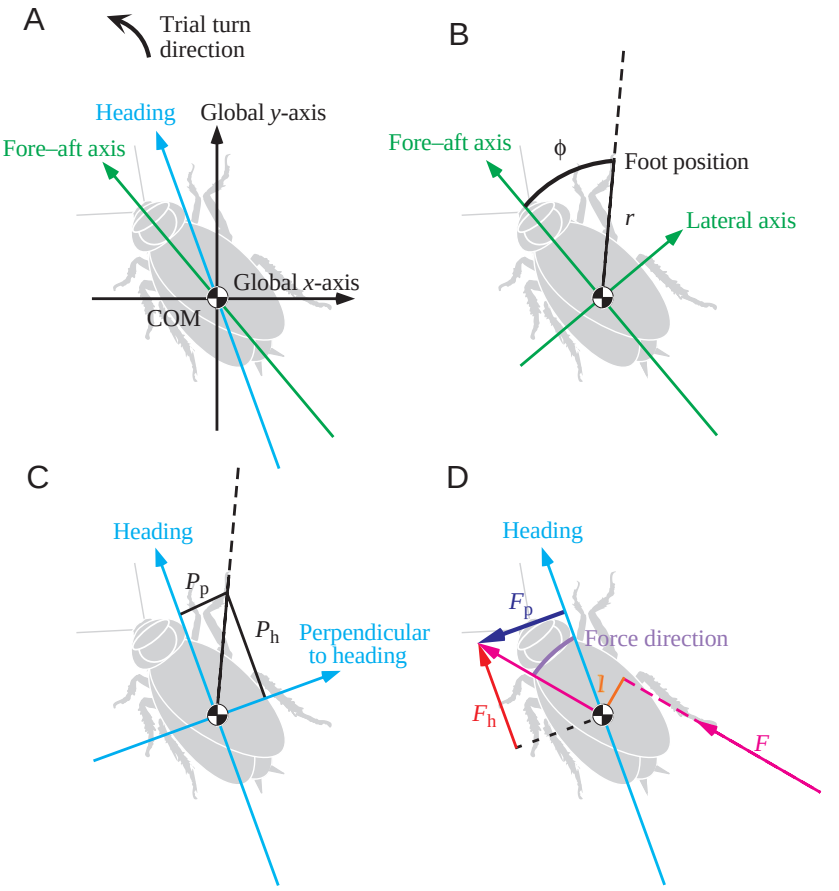

Fig. 2. (A) The three coordinate systems employed in the present study. The global *x*-axis was set by the horizontal axis of the video field. Coordinate systems based on the animal's heading and fore–aft axis were also used. (B) Measured foot placements were expressed in polar coordinates (r, ϕ) relative to the fore–aft axis, with the origin at the center of mass (COM). Green arrows indicate positive directions of the fore–aft and lateral axes. The positive lateral axis was defined to be orthogonal to the fore–aft axis and to lie in the half of the coordinate system containing the net center of rotation of the trial. (C) The heading-based coordinate system (blue arrows). One axis was chosen to lie along the heading. The direction of the axis perpendicular to the heading was defined to be orthogonal to the heading and to lie in the half of the coordinate system containing the net center of rotation of the trial. Foot location relative to heading was expressed in Cartesian coordinates. P_h is the location of the foot parallel to the heading. P_p is the location of the foot perpendicular to the heading. (D) Kinetic variables. The resultant horizontal force (F; magenta arrow) can be resolved into components parallel (F_h; red arrow) and perpendicular (F_p; blue arrow) to the heading. F_p causes the direction of movement to change (deflect). The moment arm (l) is the perpendicular distance between the COM and the line of action of the resultant force. The force direction angle was calculated relative to the heading axis.

produced by the legs on the gelatin during stance. Since the feet did not slip on the gelatin, their position remained constant during a step. We used the average of several measurements of touchdown position over the step as a constant value for foot touchdown position for subsequent analysis.

Linear velocity, linear acceleration, rotational velocity and rotational acceleration were calculated from the positions of the COM and the fore–aft axis angle. We used a fourth-order difference equation (Biewener and Full, 1992) to differentiate position measurements to yield velocity and acceleration. Curvature was calculated using three successive positions of the COM.

We selected a period of each trial (the turn duration) that contained a change in fore–aft axis angle greater than 20 ° and an integral number of steps. We did not select trials on the basis of heading deflection. The magnitude of fore–aft axis rotation (θ_r) was calculated as the difference between the fore–aft axis angle at the end of the period and the fore–aft axis angle at the beginning of the period.

Gait

We calculated phase relationships between legs during the steps of a turn by calculating the time at which a leg contacted the surface relative to the step of a reference leg normalized to the period of a reference leg (Jamon and Clarac, 1995). Phase values of 0 or 1 represent simultaneous (in-phase) stepping, and phase values of 0.5 represent alternating (anti-phase) stepping.

Foot placement

We measured foot placements at the beginning of each step (anterior extreme position; AEP) and at the end of each step (posterior extreme position; PEP) in polar coordinates (r, ϕ). The origin was placed at the COM, and ϕ was measured relative to the fore–aft axis (Fig. 2B). For comparison, we also calculated AEPs and PEPs for straight-ahead running from five three-dimensional kinematic data sets previously collected in our laboratory (Kram et al., 1997). The AEP was estimated as (r, ϕ) of the tibia–tarsus joint when the angle ϕ was minimal, and the PEP as (r, ϕ) when ϕ was maximal. We assumed that foot placement during straight-ahead running is symmetrical about the midline, and pooled the data from the right and left sides of the body, resulting in 10 measurements for each leg. Since the animals used in the present study were approximately 30 % longer than the animals in the previous study, we scaled the r components of the AEP (r_{AEP}) and the r components of the PEP (r_{PEP}) from the previous study by 1.3 when comparing them with the positions calculated during turning.

Ground-reaction forces

We used the same apparatus employed by Full et al. (1995) to calibrate the gelatin for measurements of ground-reaction force, but revised the calibration analysis. For the calibrations

used in the present study, we assumed that the intercepts of the calibration equations (equations 11 and 12 in Full et al., 1995) resulted from small asymmetries in the placement of the calibration apparatus and were not due to any inherent asymmetry of the gelatin. At zero horizontal force, the quadrant span should be zero and the quadrant ratio should be 0.5. To account for this, we did not use the intercepts of the calibration equations. Equations 11 and 12 in Full et al. (1995) thus become:

$$\sigma_h = M_1 \times \text{span} \ , \tag{1}$$

$$\frac{\sigma_h}{\sigma_t} = M_2 \times \text{ratio} \ , \tag{2}$$

where σ_h and σ_t are horizontal and total stress, respectively, and M_1 and M_2 are constants. We analyzed the optical patterns on the gelatin produced by the cockroaches using a program implemented in LabVIEW 2.2.1 with the Ultimage Concept V.i. image analysis package. Video images were analyzed in a similar method to that presented by Full et al. (1995). A small region from each image captured from video (Fig. 3A) was isolated, passed through a threshold function, manually cleared of noise caused by debris on the gelatin, and divided into four quadrants (Fig. 3B). Given the plate-specific calibration and the angle calibration presented by Full et al. (1995), forces were calculated for each foot (Fig. 3C). This process was repeated for each image, allowing us to measure the time course of force generation (Fig. 3D).

The optical patterns during complete steps deviated from the optical patterns modeled in Full et al. (1995). Discrete lobes of the 'cloverleaf' were often difficult to see at the beginning and end of the step (when the forces were smaller than during mid-stride), and patterns deviated from the expected elliptical shape even when force production was maximal for the step. In analyzing all patterns, we attempted to estimate the center of the pattern (which was made easier by considering the preceding and subsequent patterns and assuming that the point of contact was the same) and collected area and intensity values from the four quadrants surrounding the estimated center of the pattern (the origin).

When portions of the optical pattern became obscured by the body of the cockroach, we filled in the obscured area by eye or by reflecting the unobscured half of the lobe's midline to the obscured half. In cases in which the entire pattern passed under the body, we did not collect forces from the pattern during that time. These periods usually occurred at the end of a step, when forces were relatively small, and did not affect the conclusions of our analysis.

Precise foot contact areas are difficult to measure during running. We did not attempt to estimate the tarsal contact areas during running, but used the total tarsal pad areas presented in Full et al. (1995). The total tarsal pad areas used are probably larger than the area of the tarsi that actually contacted the substratum. Overestimating the contact areas causes proportional overestimation of measured forces, but would not change the measurement of the direction of the horizontal force.

The horizontal forces were large relative to the vertical forces. This caused many patterns to depart from the model presented by Full et al. (1995). Quadrants adjacent to the largest quadrant [a_I and a_{III} adjacent to a_{II}; see Fig. 7 and the associated text in Full et al. (1995) for a description of symbols a_I, a_{II}, a_{III}, a_{IV} and a_{IV}*] often summed to a value less than a_{II}, resulting in calculations of negative numbers for a_{IV}*. Since we have found that quadrant span continues to increase linearly with horizontal force even when a_{IV} drops to zero (D. L. Jindrich and R. J. Full, unpublished data), we truncated negative values of a_{IV}* to zero. Equation 8 from Full et al. (1995) was modified to:

$$a_{IV}^* = \max[(a_I + a_{III} - a_{II}),0] \ , \tag{3}$$

where a_I, a_{II} and a_{III} are areas of patterns in quadrants I, II and III, respectively.

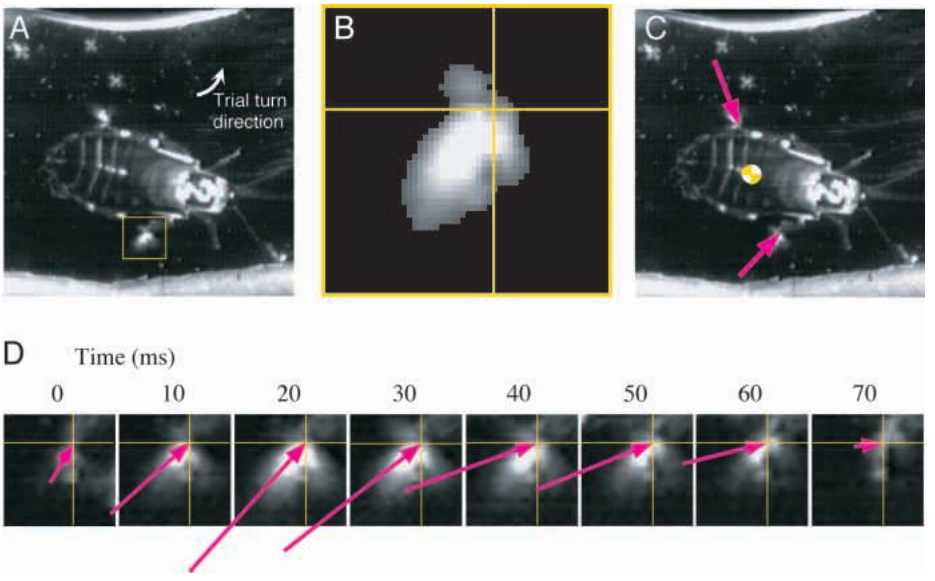

Fig. 3. Gelatin image-analysis procedure for measurements of ground-reaction force. (A) Video frame showing a cockroach turning. The yellow square frames the stress-induced optical pattern generated by the outside middle leg. (B) Optical pattern for the outside middle leg after it has been cleared of noise and passed through a threshold function. The yellow lines represent the axes used to divide the images into quadrants for analysis. (C) Optical patterns from all legs producing force were analyzed separately. Magenta arrows indicate the direction of force production. The yellow-and-white marker represents the location of the center of mass. (D) Force measurements over time. Magenta arrows show the direction and relative magnitude of forces measured for the outside middle leg. Images are presented at 10 ms intervals. Numbers above the images in D indicate the time from the beginning of the step.

Large horizontal forces also make it difficult to measure vertical forces because, in situations where horizontal forces are large enough to cause the quadrant ratio (the ratio of the larger half of the pattern to the smaller half; see Fig. 5 in Full et al., 1995) to reach 1, the vertical force becomes indeterminate and cannot be measured. Vertical forces obtained by analyzing patterns where the quadrant ratio was 1 represent estimates of minimum vertical forces. We did not use vertical force measurements in the present analysis, but this limitation should be taken into consideration in future applications of the technique.

Resultant horizontal forces calculated by the LabVIEW program were resolved into global components based on an axis of the video field. The global *x*-axis (Fig. 2A) was set to coincide with the horizontal axis of the video field (see Fig. 5 and equation 7 in Full et al., 1995). These components were filtered using a cut-off frequency of 100 Hz. The magnitude of the filtered resultant horizontal force and the force angle were then recalculated from the filtered components.

Single-leg force and torque production

We determined the contribution of individual legs to deflection of the heading by resolving the resultant horizontal force into components relative to the heading of the animal (Fig. 2D). The component parallel to the heading of the body (F_h) accelerates or decelerates the body. The component perpendicular to the heading (F_p) changes the heading direction. We calculated the perpendicular force impulse ($\Delta\mathbf{P}_{leg}$) by integrating F_p with respect to time over the duration of the step period.

We determined the contributions of individual legs to rotation of the body by calculating torque (T) about the COM produced by each leg (Fig. 2D). T was calculated as the component of the horizontal force perpendicular to the moment arm (the vector from the COM to the line of action of the force) times the length of the moment arm (l). Positive T acts to rotate the body in a counter-clockwise direction. We calculated the torque impulse generated by a single leg ($\Delta\mathbf{L}_{leg}$) by integrating T with respect to time.

We compared $\Delta\mathbf{P}_{leg}$ and $\Delta\mathbf{L}_{leg}$ among individual legs over periods limited to an integral number of strides. To control for differences in turn magnitudes, which may change the magnitudes of the total forces produced by the legs, we ranked $\Delta\mathbf{P}_{leg}$ and $\Delta\mathbf{L}_{leg}$ among the legs in a given tripod.

We calculated the mean direction of ground-reaction forces relative to the heading by resolving the resultant horizontal forces into their components F_h and F_p, averaging the F_h and F_p measurements over the course of the step, then calculating the mean force direction as $\tan^{-1}[(\text{mean } F_p)/(\text{mean } F_h)]$.

Statistical analysis

We used Mann–Whitney *U*-tests to compare variables calculated from kinematic measurements (i.e. θ_d, the force impulse in the direction perpendicular to the initial heading, $\Delta\mathbf{P}$, the torque impulse, $\Delta\mathbf{L}$, the net force and T). We compared phase relationships between leg pairs with the expected value for antiphase stepping (0.5) using unpaired *t*-tests. To compare duty factor values among legs, we conducted a nested analysis of variance (ANOVA) with leg and individual as treatments and with leg nested within individual. We used multivariate analysis of variance (MANOVA) to compare leg AEP and PEP values. r_{AEP}, r_{PEP} and the corresponding angles between the fore–aft axis and the AEP (ϕ_{AEP}) and PEP (ϕ_{PEP}) were all included as dependent variables in the analysis. To compare turning with straight-ahead running, leg and behavior (turning or straight-ahead running) were included as treatments, and the leg/treatment interaction was tested for significance. To compare contralateral sides of the body during turning, leg/side interactions were tested for significance. We used Cochran's *Q*-test (Siegel, 1956) to analyze single-leg force production frequency data and Kruskal–Wallis tests to compare leg torque impulses. We used a statistical program (StatView 4.5, Abacus concepts, Inc.) to calculate *t*-tests, Mann–Whitney *U*-tests and Kruskal–Wallis tests. We used a separate statistical program (SuperANOVA, Abacus concepts, Inc.) to conduct ANOVA and MANOVA calculations. We calculated Cochran *Q*-tests manually using a spreadsheet (Microsoft Excel).

Results

Gait

Cockroaches employed an alternating tripod gait throughout the course of a turn (Fig. 4A). Phase relationships among contralateral and ipsilateral legs were not significantly different from 0.5 (*t*-tests, $P>0.15$ in all cases; Table 1). Duty factors averaged 0.56±0.1 (mean ± S.E.M., $N=10$) and did not differ significantly between legs (MANOVA, $P=0.16$).

Velocity, curvature and body rotation

We selected trials in which the animals ran at close to their preferred speed of 20 cm s^{-1} (Full and Tu, 1990; Table 2). A trial averaged 3.6 steps. The mean duration of a single step was 69 ms. Cockroaches did not follow a constant trajectory while turning, but accelerated and decelerated during a turn (Fig. 4B,C). Heading change (θ_d) during a complete trial

Table 1. *Phase relationships among legs during turning*

	Phase
Ipsilateral legs	
Inside front in inside middle	0.53±0.09
Inside middle in inside hind	0.50±0.17
Outside front in outside middle	0.57±0.13
Outside middle in outside hind	0.45±0.08
Contralateral legs	
Inside front in outside front	0.50±0.09
Inside middle in outside middle	0.53±0.14
Inside hind in outside hind	0.52±0.06

Values are means ± S.E.M. ($N=8$).

Inside legs are expressed within the step cycle of outside legs and anterior legs within the step cycle of posterior legs.

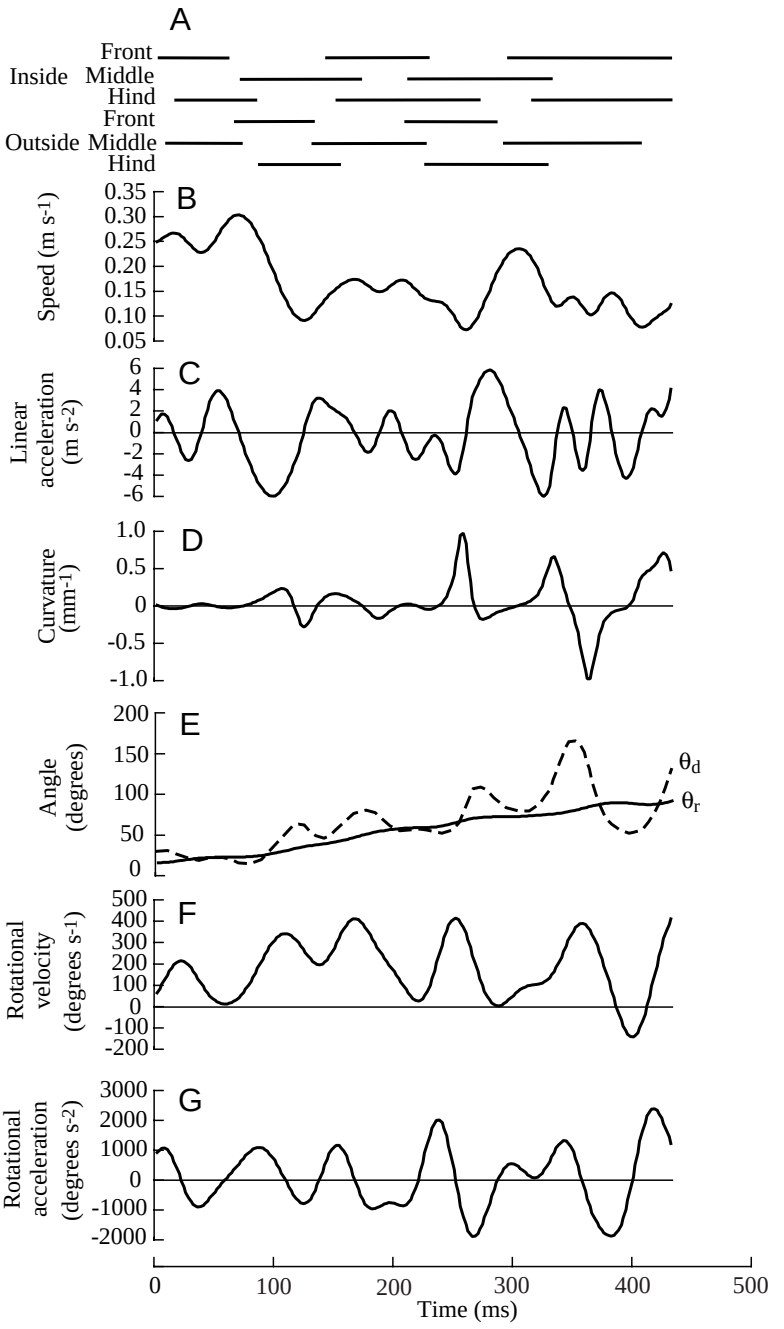

Fig. 4. Kinematics for one trial over time. (A) Gait diagram. Bars represent stance. (B) Linear speed of the center of mass (COM). (C) Linear acceleration of the COM. Positive values indicate acceleration, negative values indicate deceleration. (D) Curvature over time. Positive values of curvature indicate deflection in the trial turn direction. (E) Fore–aft axis angle (θ_r; solid line) and heading (θ_d; broken line) expressed in global coordinates. (F) Rotational velocity. Positive values indicate turning in the trial turn direction. (G) Rotational acceleration.

averaged 48 ° (Table 2). The maximum θ_d per step in the trial turn direction was not significantly different from the mean net deflection found for a complete trial (Mann–Whitney *U*, *P*=0.92; Table 2). This apparent discrepancy can be explained by the observation that, for many steps, θ_d was directed against the net deflection for the trial. Deflection in one direction tended to alternate with deflection in the opposite direction. Curvature (*1*/*R*) varied considerably within trials (Fig. 4D). Periods of relatively straight running were interspersed with periods in which the center of mass was rapidly accelerated perpendicularly, resulting in increased curvature values.

Fore–aft axis change (θ_r) ranged from a minimum of 22 ° in four steps over 230 ms to a maximum of 73 ° in five steps over 412 ms. θ_r per step ranged from 5.5 to 20.4 °. The fore–aft axis remained close to the heading (Fig. 4E), on average lagging behind the heading by 5 ° (Table 2). Rotational velocity varied within trials (Fig. 4F; Table 2). However, the direction of fore–aft axis rotational velocity did not change frequently during turns. The rotational velocity seldom decreased below zero.

Foot placement

Orientation at touch-down

The angle between foot placement at the AEP and the fore–aft axis (ϕ_{AEP}; Fig. 2B) did not differ significantly between straight-ahead running and during turning

Table 2. *Kinematics of turning in* Blaberus discoidalis

	Per trial (N=11)	Per step (N=41)		*Maximum step per trial (N=11)	
Initial velocity (m s^{-1})	0.23±0.25	0.23±0.012		0.30±0.015	
Final velocity (m s^{-1})	0.22±0.031	0.22±0.013		0.29±0.017	
Duration (ms)	263±29	69±3		85±6	
		Towards turn	Against turn	Towards turn	Against turn
Heading angle change, θ_d (degrees)	48±13.6	30±6 25	14±3 16	45±12 11	17±5 10
Fore–aft axis angle change, θ_r (degrees)	40±5	12±1 38	2±1 3	17±1 11	2±1 2
Fore–aft axis angle minus heading angle, $\Delta\theta$ (degrees)	–5±2	6±2 14	10±2 27	7±3 8	16±3 11
Curvature, 1/R (mm^{-1})	0.08±0.04	0.10±0.05 26	0.03±0.02 15	0.20±0.12 11	0.04±0.03 10
Perpendicular force impulse, $\Delta\mathbf{P}$ (mN s)	0.48±0.08	0.37±0.06 25	0.23±0.05 16	0.51±0.10 11	0.30±0.07 10
Net perpendicular force (mN)	2.15±0.48	5.45±0.85 25	3.37±0.78 16	7.93±1.46 11	4.41±1.07 10
Linear maneuverability number, LMN	0.75±0.32	0.72±0.37 25	0.45±0.26 16	1.33±0.82 11	0.66±0.41 10
Rotational velocity (degrees s^{-1})	157±15	166±13 38	32±17 3	246±17 11	16±7 2
Torque impulse, $\Delta\mathbf{L}$ (mN mm s)	–0.22±1.4	2.40±0.51 20	2.41±0.49 21	3.78±0.66 11	3.87±0.86 9
Net torque (mN mm)	0.85±4.9	37.6±8.5 20	36.6±7.2 21	58.7±11.9 11	59.3±12.4 9

Values are means ± S.E.M. for 11 trials.
N=11 for per trial or maximum per trial values, and N=41 for per step values, except where indicated by an integer beneath a value.
*Mean of the maximum value for one of the steps in a given trial.
R, radius of curvature.

(MANOVA, P=0.07; Fig. 5). ϕ_{AEP} values for contralateral legs were not significantly different from each other during turning (MANOVA, P=0.40).

Distance from the COM at touch-down

The distance from the center of mass to the foot at the AEP (r_{AEP}; Fig. 2B) for the inside hind leg was significantly shorter during turning than during straight-ahead running (1.38 cm *versus* 1.66 cm; MANOVA, P=0.046; Fig. 5). r_{AEP} for the outside front leg was significantly greater during turning (3.29 cm *versus* 2.97 cm, respectively; P=0.025), but r_{AEP} during turning was not significantly different from that for straight-ahead running for any of the other legs. r_{AEP} values for contralateral legs were not significantly different during turning (MANOVA, P=0.18).

Orientation at lift-off

The angle between foot placement at the PEP and the fore–aft axis (ϕ_{PEP}) for the outside middle leg was significantly greater during turning than during straight-ahead running (95 ° *versus* 82 °; MANOVA, P=0.027). ϕ_{PEP} values were not significantly different between turning and straight-ahead running for any other leg. However, ϕ_{PEP} values were significantly greater for all outside legs relative to the contralateral inside legs during turning (MANOVA, P<0.01 in all cases).

Distance from the COM at lift-off

The distance from the center of mass to the foot at the PEP (r_{PEP}) was significantly smaller for the inside front (2.54 cm *versus* 2.06 cm) and middle (1.91 cm *versus* 1.42 cm) legs during turning and significantly greater for the outside hind leg when compared with straight-ahead running (2.59 cm *versus* 2.16 cm; MANOVA, P<0.05 in all cases). r_{PEP} values for the outside middle and hind legs were significantly greater than for the contralateral inside legs (MANOVA, P<0.001 in both cases), but contralateral front leg r_{PEP} values were not significantly different (MANOVA, P=0.22).

Force impulse – deflection

Perpendicular impulses ($\Delta\mathbf{P}$) which deflect the heading and reflect trajectories of increased curvature (Fig. 4D) varied over

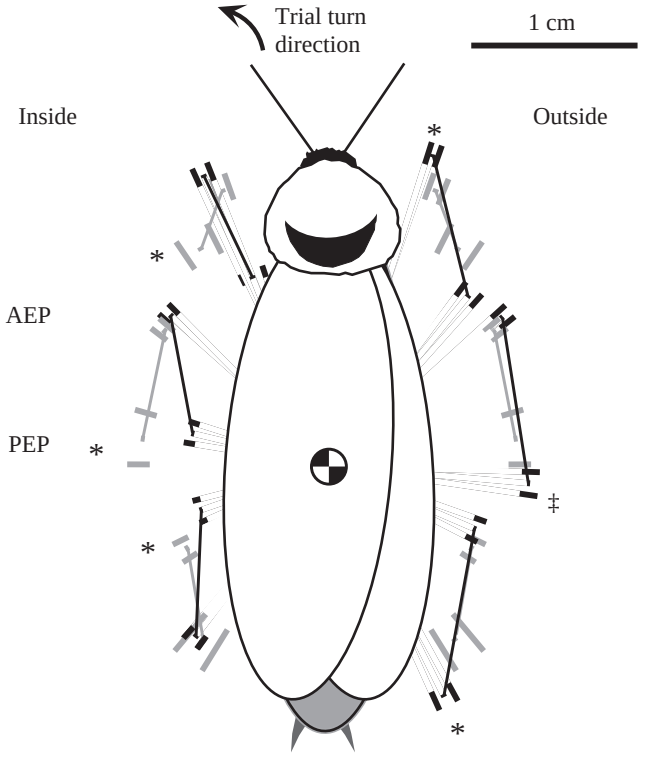

Fig. 5. Foot placement during turning (black lines) compared with straight-ahead running (grey lines). Long lines indicate the direction of leg motion relative to the fore–aft axis. Long, thin lines originate at mean anterior extreme positions (AEPs) and terminate at mean posterior extreme positions (PEPs). Shorter, thicker lines represent standard errors of the mean. The length of the short lines represents one standard error in distance (r) from the center of mass (COM). The distance of short lines from the mean value represents one standard error in direction (ϕ). An asterisk denotes a significant difference in r between turning and straight-ahead running. A double dagger (‡) denotes a significant difference in ϕ between turning and straight-ahead running. The origin is at the COM (the symbol in the center of the abdomen).

the course of a turn. A $\Delta\mathbf{P}$ which could deflect the body by as much as the total $\Delta\mathbf{P}$ observed for the entire trial could be generated in a single step (Table 2). The mean $\Delta\mathbf{P}$ for the step that generated the maximum $\Delta\mathbf{P}$ among the steps of the trial was not significantly different from the mean value per step or per trial (Mann–Whitney U, $P>0.65$ in both cases; Table 2). Greater deflection of the heading over the complete trial did not occur because steps producing 70 % of the $\Delta\mathbf{P}$ towards the turn were observed to be interspersed with steps that produced $\Delta\mathbf{P}$ against the turn (Table 2). The maximum net perpendicular force (the sum of the F_p produced by all the legs over the duration of the step) exerted on the COM per step was significantly greater than values for the complete turn (Mann–Whitney U, $P<0.001$). The net perpendicular force per step on the center of mass in the direction of the turn was also significantly greater than values for the complete turn (Mann–Whitney U, $P=0.005$; Table 2). The mean, maximum net perpendicular force during a step was 3.7 times greater than the mean value per trial (Table 2).

Table 3. *Kinematics for alternate tripods during turning*

	Inside front, outside middle, inside hind legs	Outside front, inside middle, outside hind legs
Perpendicular force impulse, $\Delta\mathbf{P}$ (mN s)		
Towards turn	0.184±0.07 6	0.429±0.07 18
Against turn	0.180±0.07 14	0.197±0.17 3
Torque impulse, $\Delta\mathbf{L}$ (mN mm s)		
Towards turn	2.71±0.94 8	2.19±0.60 12
Against turn	2.69±0.77 12	2.05±0.56 9

Values are means ± S.E.M. for 11 trials.
Integers beneath values indicate the number of steps.

The tripod consisting of the inside front, outside middle and inside hind legs generated $\Delta\mathbf{P}$ in the trial turn direction in 35 % of the steps made by this tripod (Table 3). The tripod consisting of the outside front, inside middle and outside hind legs generated $\Delta\mathbf{P}$ in the trial turn direction in 85 % of the steps made by this tripod. The mean magnitude of $\Delta\mathbf{P}$ in the trial turn direction produced by this tripod was more than twice that of the alternative tripod, resulting in a significant difference in magnitude (MANOVA, $P=0.002$).

Torque impulse – rotation

Torque impulses ($\Delta\mathbf{L}$) resulting in rotational acceleration which can alter the body angle varied over the course of a turn (Fig. 4G). Maximum $\Delta\mathbf{L}$ for a single step during a trial was significantly greater than values for the complete trial (Mann–Whitney U, $P=0.03$; Table 2). $\Delta\mathbf{L}$ per step was of similar magnitude towards and against the trial turn direction, resulting in small torque impulses per trial (Table 2). The mean net torque exerted on the body per step for steps with net torque in the trial turn direction was significantly greater than values for the complete trial (Mann–Whitney U, $P=0.001$; Table 2). As for torque impulses, net torques per step were of comparable magnitude towards and against the trial turn direction. Therefore, small net torques were produced during the complete turn (Table 2).

The tripod consisting of the inside front, outside middle and inside hind legs was associated with $\Delta\mathbf{L}$ in the trial turn direction in 40 % of the steps made by this tripod (Table 3). The tripod consisting of the outside front, inside middle and outside hind legs was associated with $\Delta\mathbf{L}$ in the trial turn direction in 57 % of the steps made by this tripod. Torque impulse magnitudes did not differ significantly during the steps of alternative tripods (MANOVA, $P=0.67$).

Single-leg force production – deflection

Individual leg forces perpendicular to the heading were

Table 4. *Single-leg force production during turning in cockroaches*

	Outside legs			Inside legs		
	Front	Middle	Hind	Front	Middle	Hind
Mean force angle (degrees)**	87±15	38±13	45±14	–119±21	–76±12	–41±8
Heading deflection						
% of steps with $\Delta\mathbf{P}_{leg}$						
Towards turn	76	85	71	20	5	10
Against turn	14	15	24	55	95	85
% greatest $\Delta\mathbf{P}_{leg}$¶						
Towards turn	43	75	57	20	0	5
Against turn	5	0	10	5	81	90
% total $\Delta\mathbf{P}_{leg}$ in trial turn direction*	90±5	99±1	87±4	61±2	0	56
Fore–aft axis rotation						
% of steps with $\Delta\mathbf{L}_{leg}$						
Towards turn	76	90	43	30	14	45
Against turn	14	10	52	45	85	50
% greatest $\Delta\mathbf{L}_{leg}$‡						
Towards turn	52	80	43	10	5	10
Against turn	10	5	14	45	71	45
% total $\Delta\mathbf{L}_{leg}$ in trial turn direction*	96±3	83±4	86±6	100±0	55	78±22
Rotational moment arm (mm)	10±2.0	9.9±1.3	1.16±1.8	–2.1±3.0	–8.9±1.33	–1.8±1.54
Leg effectiveness number§	1.05±0.12	0.48±0.06	–0.42±0.06	1.02±0.14	0.50±0.07	–0.44±0.08

Values are means ± S.E.M., except where only one value was recorded, in which case that value is indicated.

Shaded columns represent one tripod (N=21 steps), unshaded columns the alternative tripod (N=20 steps).

Percentages do not always sum to 100 because steps with undetectable force were not included.

¶Percentage of steps in which the given leg produced the largest perpendicular force impulse ($\Delta\mathbf{P}_{leg}$) relative to the other legs of its tripod.

‡Percentage of steps in which the given leg produced the largest torque impulse ($\Delta\mathbf{L}_{leg}$) relative to the other legs of its tripod.

*Percentage of the total force or torque impulse when the leg produced the greatest impulse relative to the other legs of the tripod. Percentages are relative to the sum total of the force or torque impulses in the trial turn direction produced by all the legs of a given tripod.

**Mean force angle is calculated from $\tan^{-1}\left(\frac{\text{mean } F_p}{\text{mean } F_h}\right)$, where F_p is the component of force (F) perpendicular to the heading and F_h is the component parallel to the heading. Positive values indicate that the direction of the force causes a deflection in the trial turn direction. Negative values indicate that direction of the force causes a deflection against the trial turn direction.

§Leg effectiveness numbers calculated from foot placement, step periods and forward velocities measured from kinematic data, body mass and moment of inertia estimated by geometric scaling ($m^{5/3}$), where m is body mass, of values reported for smaller *Blaberus discoidalis* by Kram et al. (1997).

directed most often towards the body (Table 4; Figs 3C, 6). Inside legs produced forces with negative angles relative to the heading direction and trial turn direction (Table 4), indicating that the inside legs directed their forces against the trial turn direction. Outside legs produced forces with positive angles, indicating that the outside legs directed their forces towards the trial turn direction.

Legs on the outside of the turn most frequently generated $\Delta\mathbf{P}_{leg}$ which acted to deflect the heading in the trial turn direction compared with legs on the inside of the turn in the same tripod (Cochran Q-test, P<0.001 for all comparisons). When the middle leg was the only leg of the tripod on the outside of the turn, it produced the greatest $\Delta\mathbf{P}_{leg}$ in the largest percentage of steps (Kruskal–Wallis test, P=0.001). When the front and hind legs were the legs of the tripod on the outside of the turn, the hind leg produced the greatest $\Delta\mathbf{P}_{leg}$ in a larger percentage of steps than the front leg (Kruskal–Wallis test, P<0.001).

One leg produced a majority of the total force impulse responsible for changing the heading of the animal. When a leg produced the largest $\Delta\mathbf{P}_{leg}$, the impulse generated by that leg averaged 79 % of the total perpendicular force impulse in the trial turn direction. For the outside legs, this impulse was significantly greater than the 33 % that would be expected if all the legs contributed equally to deflecting the body (t-tests, P<0.001 in all cases; Table 4). Inside front legs produced impulses that were significantly different from 33 % of the total perpendicular force impulse (t-tests, P<0.05). Inside middle

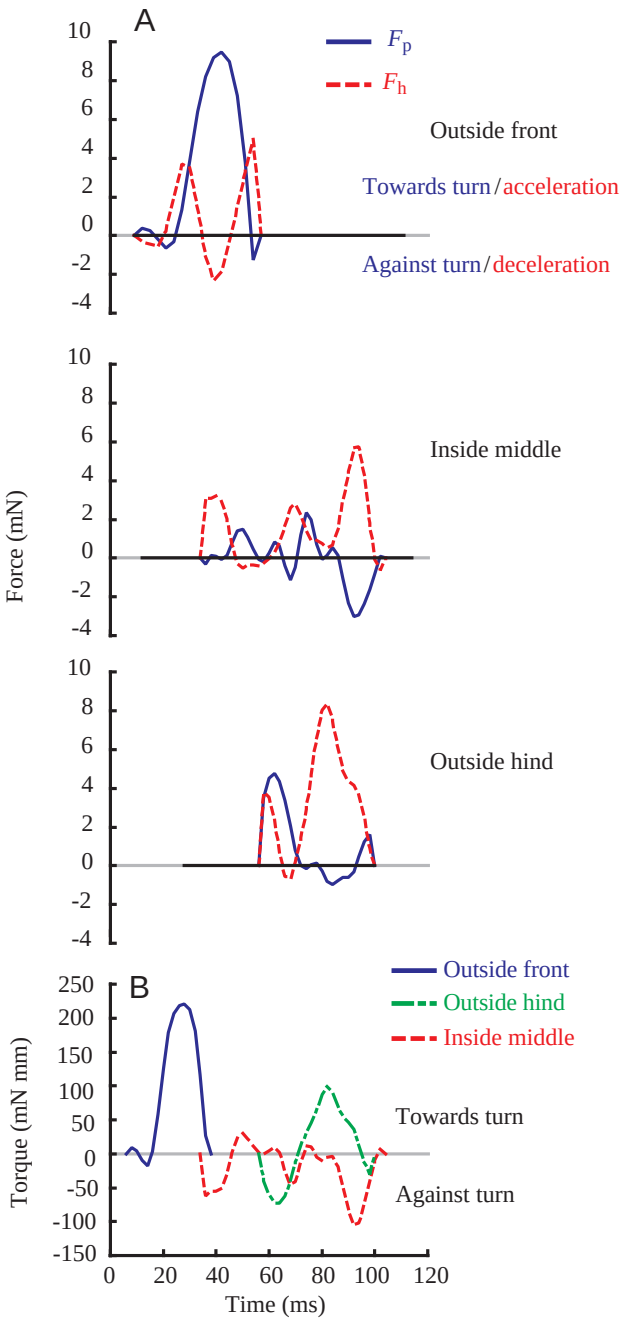

Fig. 6. Force patterns in the horizontal plane collected over the course of one step. This is an example of a step in which the outside front leg generated the largest perpendicular force impulse and the largest torque impulse. (A) Forces collected from gelatin analysis were resolved into components relative to the heading of the animal. Forces perpendicular to the heading (F_p, blue solid lines) and forces parallel to the heading (F_h, red dashed lines) are shown. Positive values of F_p indicate a force in the trial turn direction. Horizontal black lines indicate periods during which the leg contacted the substratum. During some periods when the leg contacted the substratum, force production was not detectable. (B) Rotational torques over time for the outside front, inside middle and outside hind legs. Positive torque contributes to rotation in the trial turn direction.

and inside hind legs produced force impulses that were not significantly different from 33 % of the total because of the low sample sizes for these legs.

Single-leg torque production – rotation

Legs most often produced torque that tended to rotate the body away from themselves (Table 4). Legs on the outside of the turn tended to produce positive torque rotating the body towards the trial turn direction (Fig. 6). Legs on the inside of the turn tended to produce negative torque rotating the body against the trial turn direction. The outside middle leg generated $\Delta\mathbf{L}_{leg}$ towards the trial turn direction significantly more frequently than did the outside hind leg (Cochran *Q*-test, $P<0.05$), but not significantly more frequently than the outside front leg (Cochran *Q*-test, $P>0.7$).

When the middle leg was the only leg of the tripod on the outside of the turn, it produced the greatest $\Delta\mathbf{L}_{leg}$ towards the trial turn direction in the largest percentage of steps (Kruskal–Wallis test, $P<0.001$). When the front and hind legs were the legs of the tripod on the outside of the turn, they produced the greatest $\Delta\mathbf{L}_{leg}$ towards the turn with similar frequency, but in a significantly greater proportion of steps, than the inside middle leg (Kruskal–Wallis test, $P=0.016$).

When a leg produced the largest $\Delta\mathbf{L}_{leg}$, the impulse generated by the leg averaged 83 % of the total torque impulse in the trial turn direction. This indicates that one leg produced a majority of the total torque impulse responsible for rotating the animal. For the outside legs and the inside front leg, this impulse was significantly greater than the value of 33 % that would be expected if all legs were contributing equally to deflecting the body (*t*-tests, $P<0.001$ in all cases). The inside middle and inside hind leg produced torque impulses that were not significantly different from 33 % of the total because of the low sample sizes for these legs.

Moment arms contributing to torque production for the outside front and middle legs were significantly greater than moment arms for the outside hind legs (ANOVA, $P<0.001$ for both comparisons) but were not significantly different from each other (ANOVA, $P=0.98$; Table 4). Moment arms for the inside middle leg were significantly greater than those for the front and hind legs on the inside of the turn (ANOVA, $P=0.013$ and $P=0.005$, respectively), but moment arms for the front and hind legs were not significantly different from each other (ANOVA, $P>0.9$).

Discussion

Turns during rapid running were unsteady and dynamic. Turns were characterized by periods of straight-ahead running punctuated by periods where the heading was deflected, resulting in movements of high curvature. The speed of the COM was not constant over the course of a single turn trial (Fig. 4B). Cockroaches accelerated and decelerated within each step (Fig. 4C), similar to the mechanics observed during constant average-speed, straight-ahead running (Full and Tu, 1990).

Curvature fluctuated during turning for rapid-running cockroaches (Fig. 4D), resulting in θ_d values both towards and against the trial turn direction (Table 2). Cockroaches were capable of turns with curvatures comparable with those reported for ants *Cataglyphis albicans* (typical values of 0.25 mm^{-1}, maximum of 1.5 mm^{-1}; Zollikofer, 1994), fruit flies *Drosophila melanogaster* (maximum of 0.1 mm^{-1}; Götz and Wenking, 1973) and stick insects *Carasius morosus* (0.1–0.2 mm^{-1}; Jander, 1985) moving at approximately one-tenth of the speeds used by the cockroaches in the present study (Table 2).

In contrast to the changes in heading deflection observed during turning, cockroaches maintained their rotational velocity in the trial turn direction (Fig. 4F). Only three out of 41 steps exhibited net rotational velocity against the trial turn direction (Table 2). The rotational velocities measured during turning were an order of magnitude greater than the fluctuations in rotational velocity reported for crayfish (*Procambarus clarkii*) turning at 6 $cm\,s^{-1}$ (Domenici et al., 1998). Unlike cockroaches, the rotational velocities observed in crayfish fluctuated around zero. Rotational velocity in cockroaches fluctuated within steps due to $\Delta\mathbf{L}$ both towards and against the trial turn direction. The observed torque impulses were due to large fluctuations of rotational acceleration throughout turns (Fig. 4G). However, $\Delta\mathbf{L}$ against the trial turn direction was similar to $\Delta\mathbf{L}$ in the trial turn direction, causing a positive rotational velocity to be maintained throughout the turn. Rotational acceleration also alternates direction within steps during straight-ahead locomotion (Full and Tu, 1990; Kram et al., 1997), but rotational velocity fluctuates around a value of zero.

Cockroaches performed turns of magnitudes similar to those of other insects moving at approximately one-tenth of the speeds used in the present study. The magnitudes of fore–aft axis rotation that we measured for turning cockroaches (5–20 ° per step; Table 2) were comparable with the rotation magnitudes measured in the same species during slow running (15–30 ° per step; Watson and Ritzmann, 1998) and those measured in stick insects moving at approximately 0.5–2 $cm\,s^{-1}$ (10–20 ° per step; Jander, 1985). More rapid turns have been described in American cockroaches (*Periplaneta americana*) during escape turning. *Periplaneta americana* can rotate by 90 ° initially over the course of one stride period (Camhi and Levy, 1988) and can execute alternating turns at frequencies of 25 Hz (Camhi and Johnson, 1999). The turns we measured can be considered as turns of moderate magnitude and are most certainly not the maximum performance of these animals.

Despite the dynamic nature of turning, cockroaches maintained their fore–aft axis close to the direction of their heading (Fig. 4E). The magnitude of heading deflection for the entire trial (48 °) matched the magnitude of fore–aft axis rotation (40 °). The mean value of $\Delta\theta$ throughout the turns was only 5 ° (Table 2).

Turning dynamics can be characterized as a minor modification of straight-ahead running

Cockroaches decelerated and accelerated both in speed and in rotational velocity during turning, typical of the bouncing gait observed during straight-ahead running (Full and Tu, 1990; Kram et al., 1997). Minor alterations in the perpendicular force impulses and rotational torque impulses produced by cockroaches during straight-ahead running could account for the whole-body mechanics observed during turning (Fig. 7). Heading deflection resulted from a decrease in $\Delta\mathbf{P}$ relative to straight-ahead running by the tripod containing the outside middle leg and from instances of $\Delta\mathbf{P}$ production in the direction opposite to that observed during straight-ahead running (Table 3). Both effects could result from an increase in force production or stiffness of the outside middle leg. Body rotation resulted from both tripods deviating from straight-ahead running by producing non-zero values of $\Delta\mathbf{L}$ during a step.

Force impulse

The tripod containing the inside middle leg was responsible for the majority of $\Delta\mathbf{P}$ and $\Delta\mathbf{L}$ production in the trial turn direction. This tripod produced $\Delta\mathbf{P}$ in the trial turn direction in 18 steps and $\Delta\mathbf{L}$ in the trial turn direction in 12 steps of the 21 steps observed (Table 3). During turning, this tripod produced $\Delta\mathbf{P}$ in the same direction and of approximately equal magnitude to the $\Delta\mathbf{P}$ expected during straight-ahead running. As for straight-ahead running, $\Delta\mathbf{P}$ was directed towards the middle leg in a majority of steps (Fig. 7). Even though the tripod containing the inside middle leg generated the largest $\Delta\mathbf{P}$ in the trial turn direction, this $\Delta\mathbf{P}$ was only 25 % greater than the $\Delta\mathbf{P}$ observed during straight-ahead running. The force impulses observed during straight-ahead running are sufficient to generate turns of magnitudes comparable with those measured in the present study.

The tripod containing the outside middle leg generated $\Delta\mathbf{P}$ in the trial turn direction (in the direction away from the middle leg) in six out of 20 steps (Table 3). The tripod containing the outside middle leg thus also contributed to deflecting the heading in the trial turn direction. The direction of $\Delta\mathbf{P}$ production during these steps represents a departure from the $\Delta\mathbf{P}$ exhibited during straight running, which is directed towards the middle leg (Full et al., 1991; Full and Tu, 1990). The tripod containing the outside middle leg produced $\Delta\mathbf{P}$ in the trial turn direction of approximately half the magnitude of the alternative tripod. Force impulses produced by this tripod against the trial turn direction were also nearly half those expected during straight-ahead running. The shift in $\Delta\mathbf{P}$ production by the tripod containing the outside middle leg could result from a decrease in force production by the inside front or hind legs, from an increase in force production by the outside middle leg, or from both.

Torque impulse

The tripod containing the inside middle leg generated $\Delta\mathbf{L}$ in the trial turn direction in a majority of steps (Table 3). This resulted from the fact that both tripods generated torque impulses in the direction of their middle leg more frequently than in the opposite direction. The magnitudes of the torque impulses within single steps during turning were greater than

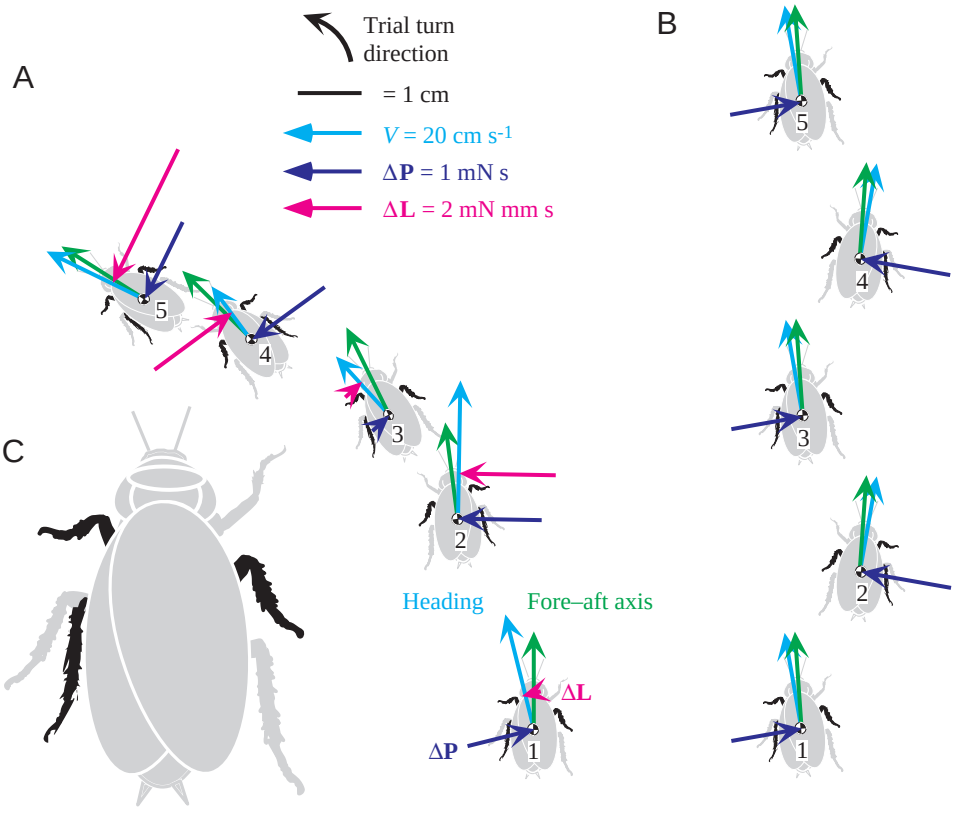

Fig. 7. Kinematics and whole-body kinetics during turning and straight-ahead running. Heading (light blue arrow representing the velocity vector of the center of mass, COM), fore–aft axis direction (green arrow) and the position of the COM at the beginning of the step (symbol in the center of the abdomen) are shown. Darkened legs indicate legs in stance. Drawings of animals in A and B are scaled to approximately one-sixth of their length in the length scale of the figure for clarity (see C for a cockroach in the length scale of the figure). Perpendicular force impulses (Δ**P**, dark blue arrows perpendicular to the heading and directed through the COM) and torque impulses (Δ**L**, represented by magenta arrows perpendicular to heading axis, arbitrarily located anterior of the COM for clarity) represent Δ**P** and Δ**L** over the duration of the subsequent step, when the darkened legs are in stance. (A) A turning trial in which an animal turns to the left. In all steps except 5, Δ**P** was directed towards the middle leg, causing the heading to deflect in the direction of the middle leg in stance. Δ**L** is directed both towards and against the trial turn direction. The fore–aft axis rotated in the trial turn direction in every step because a positive rotational velocity was maintained over the duration of the turn (see Fig. 4F). (B) Straight-ahead running at a constant speed of 20 cm s^{-1}. Perpendicular force impulses within each step are directed towards the middle legs in stance, causing the heading to deflect in the direction of the middle leg in stance. Torque impulses over steps during straight-ahead running are zero and, consequently, are not shown. However, cockroaches yaw towards the middle leg in stance. Force impulses and the kinematics of straight-ahead running were estimated from measurements reported by Full et al. (1991), Full and Tu (1990) and Kram et al. (1997). Note the similarities between turning and straight-ahead running. Despite turning, the position of the heading relative to the fore–aft axis was maintained during each step. In all but turning step 5, Δ**P** during turning acted in the same direction as during straight-ahead running. (C) Approximate size of a cockroach in the length scale of the figure.

those during straight-ahead running (Fig. 7). During straight-ahead running, values of Δ**L** over single steps are close to zero since rotational velocity reaches zero at step transitions (Kram et al., 1997). Torque towards the middle leg in the first half of the step causes rotation towards the middle leg, but the rotational acceleration caused by this torque is cancelled by torque against the direction of the middle leg in the second half of the step. The opposing torques within each step during straight-ahead running result in zero net torque impulses over the entire step.

During turning, torque impulses in both directions did not oppose each other equally within individual steps, resulting in both tripods producing Δ**L** towards and against the trial turn direction. Non-zero torque impulses by both tripods may act to maintain a positive rotational velocity over the duration of the turn (Fig. 4F; Table 2). As for straight-ahead running, in a majority of steps during turning, both tripods generated torque impulses that would act to rotate the fore–aft axis towards the middle leg if the rotational velocity were zero at the beginning of the steps (Table 3).

Turn kinematics were similar to straight-ahead running

The stride frequencies, duty factors and leg phases used during turning were similar to those during straight-ahead running at the same average speed. The mean stride frequency measured during turning of 7.3 Hz is similar to those reported for the same species during straight-ahead running (8–10 Hz; Full and Tu, 1990; Ting et al., 1994). Duty factors during turning averaged 0.56, similar to those reported for straight-ahead locomotion in *Blaberus discoidalis* (0.6; Ting et al., 1994).

The phase relationships found in cockroaches during turning show that cockroaches maintained a strict alternating tripod gait (Table 1), as observed during rapid straight-ahead running. Cockroaches did not turn by altering stride frequency on one side of the body relative to the other side. This is not surprising considering that cockroaches would have to nearly double their stride frequency on one side of the body relative to the other to produce the turns measured in the present study. Turning without altering stride frequency is common among arthropods moving at a range of speeds. Fruit flies *Drosophila*

melanogaster (Strauß and Heisenberg, 1990), 12 species of ants (Zollikofer, 1994) and beetles *Geotrupes stercorosus* (Frantsevich and Mokrushov, 1980) have also been found to turn during walking without altering their stride frequency. *Carausius morosus* nymphs (Graham, 1972) and adults in gradual turns (Jander, 1985) also maintain tripod gaits during turning. Similarly, tethered crayfish (*Astacus leptodactylus*) (Cruse and Silva Saavedra, 1996), stationary cockroaches *Blattella germanica* (Franklin et al., 1981) and spiders *Metaphidippus hartfordi* (Land, 1972) turn without altering the step frequency on one side of the body. Cockroaches rotating in place have a tendency towards tripod coordination (Franklin et al., 1981). Strict tripod coordination might be expected in rapid locomotion, where centrally generated, feedforward commands have been predicted to become more important in locomotory control (Pearson, 1972).

Kinematics of turning did not predict the full dynamics

Foot placement and leg movements of turning cockroaches could not be related unambiguously to leg force or torque production. Kinematic studies of maneuvers in insects frequently infer the patterns of force production and the contributions of legs to accelerating the body from the movements of the legs relative to the body in free or constrained conditions. This has led to the hypothesis that all the legs contribute to escape turning (Camhi and Levy, 1988; Schaefer et al., 1994; Tauber and Camhi, 1995). The assumption that all the legs can contribute to maneuvers is supported by the finding that any of the legs can contribute to turning the body if other legs are removed (Götz and Wenking, 1973). However, leg movements do not necessarily reflect the magnitudes of forces produced by the legs, and animals can execute turns that appear kinematically similar yet require very different amounts of force and torque production (Land, 1972). In addition, when turning during forward running, it has been noted that leg movements can result from the movement of the body over the legs and not from active force generation by the legs themselves (Domenici et al., 1998). In contrast to the movements of the feet relative to the body during the stance period, the placement of the feet at touch-down (r_{AEP} and ϕ_{AEP}) relative to the body does not depend on the movements of the body over the substratum. Changes in foot placement could therefore indicate active alterations of leg kinematics involved in turning (Cruse and Silva Saavedra, 1996). For example, Franklin et al. (1981) found that pure rotation involved measurable changes in AEP angles.

During rapid running in cockroaches, turning resulted from changes in force production among the legs that were not related to measurable differences in foot placement kinematics or in movements of the legs relative to the body during stance.

The orientation of the legs at the AEP (ϕ_{AEP}) did not differ from scaled values for straight-ahead running (Fig. 5). Functional lengths (r_{AEP}) differed from straight-ahead running for only two legs, one of which (the outside front leg) contributed to turning the body and one of which (the inside hind leg) did not. Most of the legs showed no significant differences from straight-ahead running or from the contralateral leg, whether or not the leg contributed to turning the body. This finding is similar to measurements on crayfish (*Astacus leptodactylus*), which also did not alter their AEP positions during turns (Cruse and Silva Saavedra, 1996). Consequently, kinematic changes in leg placement at the AEP did not uniquely determine leg force or torque production during turning.

Differences in ϕ_{PEP} and r_{PEP} values between legs indicate that leg excursions did differ from values for straight running and differed between contralateral legs during turning (Fig. 5). Differences in leg excursions between contralateral legs were consistent with the requirements for altering stride length on the outside of the body imposed when turning at a constant stride frequency and duty factor. Large differences in r_{PEP} relative to straight running for the inside front and middle legs might suggest that these legs were actively involved in turning. However, the inside legs actively pushed against the trial turn direction in the majority of steps (Table 4). In addition, measurable force production by individual legs did not always last for the duration of the stance period (Fig. 6), further complicating the relationship between stride kinematics and leg force production. Legs can remain in contact with the substratum and undergo large excursions but still only produce force for part of the stance period.

Contributions of outside front, middle and hind legs to turning

Since three legs contact the substratum at any one time, the individual leg forces that cause the $\Delta\mathbf{P}$ and $\Delta\mathbf{L}$ that deflect the heading and rotate the body are indeterminate. Estimating force and torque production using kinematic data was not possible since kinematics do not uniquely determine force or torque production.

Single-leg force measurements showed that, during turning, F_p for all legs was directed towards the fore–aft axis and heading axis. The inside legs pushed outwards, against the trial turn direction (Table 4). Consequently, legs on the outside of the turn generated the force and torque impulses necessary to turn the body.

Role of outside front legs

In many steps, the outside front legs contributed substantially to deflecting and rotating the body, resulting in large deflecting forces and rotational torques (Fig. 6). The outside front legs generated the greatest $\Delta\mathbf{P}_{leg}$ and $\Delta\mathbf{L}_{leg}$ in approximately half the trials (Table 4). Low force production relative to the hind legs in some steps prevented the outside front legs from generating the greatest $\Delta\mathbf{P}_{leg}$ in the trial turn direction. In spite of low force production relative to the hind legs, the outside front legs produced the greatest $\Delta\mathbf{L}_{leg}$ in the trial turn direction in a majority of steps (Table 4).

Role of outside middle legs

The outside middle legs generated the greatest $\Delta\mathbf{P}_{leg}$ and $\Delta\mathbf{L}_{leg}$ in the trial turn direction in approximately 80 % of the steps of this tripod. The tripod containing the outside middle

leg generated $\Delta\mathbf{P}$ and $\Delta\mathbf{L}$ in the trial turn direction with lower frequency than the alternative tripod (Table 3). However, the action of the outside middle leg may have been important in reducing the $\Delta\mathbf{P}$ and $\Delta\mathbf{L}$ produced by this tripod and in causing $\Delta\mathbf{P}$ to be directed in the trial turn direction in 30 % of steps and $\Delta\mathbf{L}$ to be directed in the trial turn direction in 40 % of steps.

The shift in $\Delta\mathbf{P}$ production by the tripod containing the outside middle leg could be due to a decrease in force production by the inside front or hind legs, to an increase in force production by the outside middle leg, or to both. Our data are consistent with the findings of Watson and Ritzmann (1998), which show electromyographic frequencies for outside middle legs that are greater than values recorded during straight-ahead running.

Role of outside hind legs

Outside hind legs generated the greatest $\Delta\mathbf{P}_{leg}$ among the legs of the tripod in a majority of steps because the large forces had large components perpendicular to the heading (Table 4). Despite high force production, the hind legs did not generate the greatest $\Delta\mathbf{L}_{leg}$ in a majority of steps. The large forces produced by the hind legs were associated with small moment arms (approximately 1 mm; Table 4), indicating that the forces were, on average, directed towards the COM. This resulted in small torques about the COM.

Relationship between turning dynamics and morphology and behavior

Interpretation of the complex dynamics of turning requires a simple horizontal plane model. Our model assumes that three legs of a tripod act as a single leg. Using this simple model allows patterns of leg force production to be related to the morphology of the animal (i.e. the body shape and leg position). The efficacy of a single leg in deflecting and rotating the body can be evaluated as a function of its position.

Deflection – a change in heading

An animal must deflect its heading by θ_d from its initial direction during straight-ahead running to point in a new direction (Fig. 1A). The degree of this deflection depends on $\Delta\mathbf{P}$ relative to the forward momentum of the center of mass (the product of body mass m and forward speed V). The turning performance of an animal can thus be expressed as a 'linear maneuverability number' (LMN):

$$\mathrm{LMN} = \frac{\Delta\mathbf{P}}{mV} \approx \frac{\int_{t=0}^{t=\tau} F_p \mathrm{d}t}{mV}, \qquad (4)$$

where t is time and τ is step period. In the present study, we calculated LMN as $\Delta\mathbf{P}$ relative to the initial heading divided by the initial momentum of the COM (Table 2). The integrated force perpendicular to the heading divided by the initial momentum of the COM is only approximately equal to the LMN, since the heading (and thus the direction of F_p) changes over the course of the turn. A greater total perpendicular force exerted by the legs or an increased time during which the force is produced will increase the LMN and cause a larger θ_d, since $\theta_d \approx \tan^{-1}(\mathrm{LMN})$. θ_d is only approximately equal to $\tan^{-1}(\mathrm{LMN})$ because changes in velocity in the initial movement direction over the course of the turn can change θ_d. Greater body mass or forward velocity for the same perpendicular impulse will decrease the LMN and cause a smaller θ_d.

The cockroaches in the present study were able to generate perpendicular force impulses comparable to three-quarters their linear momentum, as indicated by their LMN of 0.75 (Table 2). For comparison, a circular track would need to have a radius of curvature (R) of 3–4 m to require similar performance from a 60 kg human running at 5 m s^{-1} with a stance period of 500 ms. This would represent near-maximal performance for a human (Greene, 1985).

If the animal moves along a circular curve, the force relative to the direction of motion (F_p, the centripetal force) required to deflect the COM has a constant magnitude, mV^2/R. Other patterns of force production, which do not result in curved trajectories, are also possible.

Rotation – aligning the fore–aft axis with the heading at the end of the turn

A second requirement for a successful turn involves rotating the fore–aft axis so that it aligns with the direction of the velocity vector (Fig. 1B). Minimizing the degree of misalignment ($\Delta\theta$) between θ_d and θ_r is important for resuming straight running following a turn. To rotate its body, the animal must generate a net torque (T) about the COM. Assuming that the rotational velocity (ω) is zero at the beginning of the turn, to minimize the net $\Delta\theta$ at the end of the turn, the double integral of net angular acceleration (i.e. T divided by the yaw moment of inertia, I) with respect to time over a step period must equal θ_d. In the simplest case of a constant net torque over time, the body will have a positive ω at the end of the turn, which must be arrested in subsequent steps. We will not consider other possible cases, such as using time-varying net torque production or constraining foot placement to maintain ω=0 at the end of the turn.

Turning around a circular trajectory using a single 'effective' leg – a model

Many-legged terrestrial animals must generate net forces and torques on the COM by pushing or pulling against the substratum with their legs. A leg used to generate the perpendicular force impulse necessary to change the heading of the body may not be in an advantageous position to simultaneously generate a torque impulse to rotate the body in the appropriate direction. For example, if a leg located behind the COM (e.g. the hind legs in cockroaches) exerted a purely perpendicular force to deflect the heading, the torque resulting from this force would cause the body to rotate in the direction opposite to the direction of deflection, causing the fore–aft axis and heading to become misaligned.

The present model assumes that animals produce forces

perpendicular to the heading necessary to deflect the body using one leg initially placed at a set distance from the COM. The model allows calculation of the forces parallel to the heading necessary to rotate the body to keep the fore–aft axis aligned with the heading at the end of the step period, τ. Important simplifying assumptions of the model are as follows: (1) the heading and fore–aft axes are initially coincident with the *x*-axis of the global reference frame; (2) the animal's COM moves around a circular trajectory by generating a constant force perpendicular to the heading (F_p) using one leg placed at an initial distance in the initial heading direction ($P_{AEP,ih}$) from the COM; (3) the animal maintains an approximately constant speed (V) over the course of the turn; (4) the leg moves approximately parallel to the heading over the course of the turn; and (5) the turn begins with zero angular velocity, ω.

If F_p is constant and sufficient to deflect the animal through an angle θ_d over the step period τ, and is generated by one leg initially placed at $P_{AEP,ih}$, it will generate a torque about the COM over time that will cause the body to rotate. For $\omega=0$ initially, the animal will rotate through some angle θ_p, depending on the animal's moment of inertia, I. θ_p may not equal θ_d. The torque generated by the perpendicular force may under-rotate the body ($\theta_p<\theta_d$) or over-rotate the body ($\theta_p>\theta_d$). The relationship between θ_p and θ_d will determine whether changes in the pattern of perpendicular force production or additional force production in the heading direction may be necessary to minimize net $\Delta\theta$ over the step. The ratio of θ_p to θ_d provides an indication of how effective a leg placed at $P_{AEP,ih}$ will be in minimizing net $\Delta\theta$ given τ, m, V and I:

$$\varepsilon = \frac{\theta_p}{\theta_d} = \frac{mV\tau}{2I}\left(P_{AEP,ih} - \frac{V\tau}{3}\right), \quad (5)$$

which we term the 'leg effectiveness number' ε (see Appendix). ε measures the degree to which rotation matches deflection under the constraint of the perpendicular impulse necessary for deflecting the heading and the morphology of the animal, including the initial leg placement. Values of ε close to 1 indicate that the leg is in a favorable location to rotate the body by simply generating the perpendicular force necessary for deflection. If ε is less than 1 but greater than zero, the perpendicular force necessary for deflection rotates the body in the direction of θ_d, but is insufficient to rotate the body so that rotation matches deflection. If ε is less than zero, the rotation produced by the leg will rotate the body in the direction opposite to θ_d. If ε is greater than 1, the perpendicular force causes an over-rotation of the body.

For $\varepsilon<1$ or $\varepsilon>1$, force parallel to the heading (F_h) at a perpendicular distance of the foot from the COM (P_p) may compensate for under-rotation or over-rotation caused by F_p. At a given $\varepsilon\neq1$, θ_d, τ and I, the product of F_h and P_p necessary to minimize net $\Delta\theta$ is constant:

$$F_h P_p = K\,. \quad (6)$$

Equation 6 indicates that for a given value of ε, the F_h necessary to prevent under-rotation or over-rotation of the body is directly proportional to the placement of the leg perpendicular to the heading. The leg placement determines the amount of force parallel to the heading necessary to minimize net $\Delta\theta$. Fig. 8 shows that, for cockroaches, as the initial leg placement moves farther from the fore–aft axis (as $|P_p|$ increases), the model predicts that the required F_h decreases. The resultant force vectors change direction to become closer to being perpendicular to the heading.

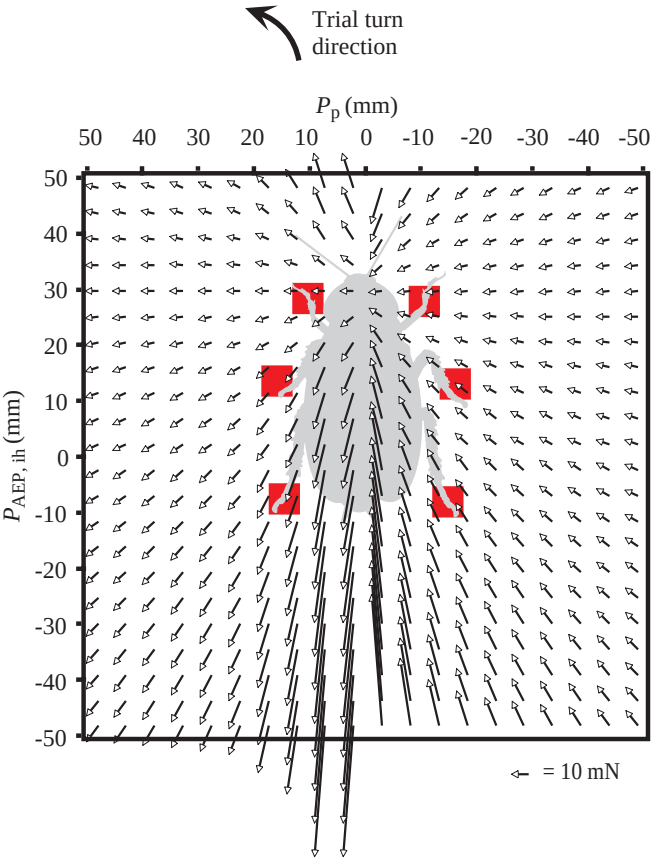

Fig. 8. Force vectors necessary to turn with net misalignment between the fore–aft axis and the heading ($\Delta\theta$) of zero as a function of initial leg position. The animal is oriented vertically (the positive fore–aft and heading directions point up the page). Red squares indicate approximate initial foot positions for the front, middle and hind legs. Body mass (m) 5 g; moment of inertia (I) 7.72×10^{-07} kg m^2 (geometric scaling, $m^{5/3}$, of values reported for smaller *Blaberus discoidalis* by Kram et al., 1997); speed of the center of mass (V) 0.20 m s^{-1}; step period (τ) 60 ms; angular change of heading (θ_d) 20°. P_p, location of the foot in the direction perpendicular to the heading; $P_{AEP,ih}$, initial location of the foot in the initial heading direction at the beginning of a step.

For a given m, V, I, θ_d, P_p and τ, the force in the heading direction necessary to minimize net $\Delta\theta$ is also directly proportional to the initial position of the foot parallel to the heading:

$$K_1 F_h - K_2 P_{AEP,ih} = 1\,, \quad (7)$$

where K_1 and K_2 are constants. Equation 7 suggests that, for

cockroaches, as the initial placement of the leg shifts posteriorly (decreasing $P_{AEP,ih}$), the force in the heading direction should increase proportionally. This is illustrated by the larger force vectors, increasingly aligned with the fore–aft axis towards the rear of the animal in Fig. 8. The Appendix describes the derivation of equations 6 and 7.

The total force predicted to turn the body is a nonlinear function of $P_{AEP,ih}$ and P_p (Fig. 8). The predicted total forces for the outside legs required to turn the body (6–15 mN) are similar to the total horizontal forces predicted for single legs of the animal during straight-ahead running (8–10 mN; scaled from single-leg forces reported in Full et al., 1991, to take the larger mass of the animals in the present study into account). However, the forces required are approximately one-tenth the maximum single-leg forces that these animals are able to produce (over 100 mN; Full and Ahn, 1995; Full et al., 1995).

Equations 6 and 7 suggest that all legs could contribute to deflecting and rotating the body. Table 4 shows that front legs are predicted to operate at an ε close to 1, indicating that the F_p required to deflect the heading should also be appropriate to rotate the fore–aft axis to minimize net Δθ. The middle and hind legs could also deflect and rotate the body to turn, but these legs operate at ε<1 and, consequently, must generate larger F_h and thus larger total forces.

Effects of leg position on the force production necessary to execute a turn

The model expressed by equations 5–7 predicts leg force production for the outside legs. At an initial ω of zero, the model predicts that the front legs should produce almost purely perpendicular forces (ε close to 1; Table 4) and that the middle and hind legs should generate acceleratory forces (ε<1; Table 4).

Efficacy of front legs

The outside front legs operate at an ε of approximately 1 (Table 4). The front legs are predicted to be effective at rotating the body simply by generating the perpendicular forces necessary to deflect the body. The force angle predicted from the ε of the front legs is 93 ° (assuming a 5 g animal turning in 60 ms with the average initial foot placements shown in Fig. 8). The mean direction of force production measured during turning for the front legs was 87±15 ° (mean ± S.E.M.; Table 4), indicating that cockroaches turned by generating nearly perpendicular forces with their front legs.

Efficacy of middle legs

The mean direction of force production for the outside middle legs was 38±13 ° (mean ± S.E.M.; Table 4). The middle legs generated large forces parallel to the heading, causing the force angle to decrease relative to the front legs. The middle legs operate at an ε of 0.48, indicating that the perpendicular forces necessary to deflect the heading rotate the fore–aft axis in the correct direction, but do not result in adequate rotation to maintain the fore–aft axis aligned with the heading at the end of the turn. The force direction predicted for the middle legs, given an ε of 0.48, is 51 °, slightly higher than the observed force direction.

Efficacy of hind legs

The mean direction of force production for the outside hind legs was 45±14 ° (mean ± S.E.M.; Table 4). The hind legs also generated large forces parallel to the heading, causing the force angle to decrease relative to the front legs. This was due to the fact that the hind legs operate at an ε of approximately −0.4, indicating that the perpendicular forces produced by the hind legs act to rotate the body against the turn direction. The force direction predicted for the hind legs, given an ε of −0.42, is 22 °, slightly lower than the observed force direction.

Turning can result from minor alterations in leg forces produced during running

The front legs produced forces nearly perpendicular to the heading direction, and the middle and hind legs produced additional forces in the heading direction. These changes in force direction are consistent with the predictions of the turning model. The moment of inertia of cockroaches is large enough relative to their body mass to require that the front legs produce almost completely perpendicular forces, and that the middle and hind legs produce large acceleratory forces, to maintain the fore–aft axis aligned with the heading at the end of the turn. The force directions predicted by the model and observed in cockroaches could result from minor alterations in the forces produced during straight-ahead running. During straight-ahead running, the front, middle and hind legs have mean directions of ±134 °, ±90 ° and ±33 °, respectively (force directions calculated from force maxima reported in Full et al., 1991). The directions of force production by the inside legs (−119 ° for the front legs, −76 ° for the middle legs and −41 ° for the hind legs; Table 4) are closer to the values observed during straight-ahead running than the values for the outside legs. Although we cannot determine whether the inside legs change the magnitudes of their force production, the direction of force production by the inside legs remained similar to the force directions during straight-ahead running. This suggests that turning resulted from changes in the direction of force production by the outside legs.

Lateral force impulses observed during straight-ahead running are sufficient to generate the perpendicular force impulses observed during turning. However, the torque impulses observed during straight-ahead running do not generate rotations sufficient to maintain the fore–aft axis aligned with the heading. To generate additional fore–aft axis rotation, cockroaches could simply reduce the deceleratory forces parallel to the heading direction produced by the front legs and increase the acceleratory forces parallel to the heading direction produced by the middle and hind legs. As a result, force direction angles for all legs should decrease relative to straight-ahead running. This is consistent with the force direction angles observed for the front and middle legs during turning, which are, respectively, 47 ° and 52 ° smaller than those observed during straight-ahead running. The hind legs,

which did not generate the majority of $\Delta\mathbf{L}$, showed mean force direction angles 12° greater than those observed during straight-ahead running. However, the mean force direction angle during straight-ahead running was only 11° greater than the force direction predicted from the leg effectiveness number of the hind legs during turning. The direction of force produced by the hind legs was only 23° greater than the force direction predicted to minimize net $\Delta\theta$.

The line containing the predicted resultant force vector intersects the fore–aft axis at a point forward of the center of mass (Fig. 8). This point is analogous to the attachment point of a single effective 'leg spring' that can model the dynamics of hexapodal locomotion in the horizontal plane (J. Schmitt and P. Holmes, in preparation). Turning with this single effective 'leg spring' is greatly facilitated by moving the attachment point forward of the center of mass, similar to the prediction of the present model.

Implications for control

Our study of maneuverability in cockroaches has shown that a many-legged, sprawled-posture morphology provides a range of immediately available options for maneuvering. The front, middle and hind legs on either side of the body could contribute to turning the body. The front legs operate at a leg effectiveness number of approximately 1, indicating that they can contribute effectively to turning by producing forces nearly perpendicular to the heading. The middle and hind legs operate at leg effectiveness numbers of less than 1, indicating that they must produce additional forces parallel to the heading, which accelerate or decelerate the animal.

The cockroaches used only a subset of the options available to them for deflecting and rotating the body. During rapid running, they used only their outside legs to generate the perpendicular forces and rotational torques necessary to deflect their heading and rotate their fore–aft axis in the trial turn direction. The inside legs acted against the turn, constraining the turning performance.

The perpendicular force impulses observed during straight-ahead running are sufficient to generate turns of the magnitudes we observed when unarrested by subsequent steps. Moreover, the single-leg ground-reaction forces predicted to turn the body based on the leg effectiveness number and the single-leg forces actually observed during turning were similar to the patterns of leg force production observed during straight-ahead running. Consequently, our analysis has revealed that the patterns of force production observed in these sprawled-postured hexapods during straight-ahead running provide the possibility for remarkable maneuverability, while requiring only minor adjustments in leg force production. The morphological design of these organisms (i.e. the leg number, leg position, mass and moment of inertia), coupled with their locomotion dynamics during straight-ahead running, could considerably simplify the control of maneuvers such as turning.

The mechanical consequences of using the front, middle or hind legs to turn have potential applications to simplifying the control of maneuvers under different conditions. The front legs are in an advantageous position to turn the body while minimizing net $\Delta\theta$ when initiating a turn from a rotational velocity close to zero. In addition, the front legs can contribute to turns without accelerating or decelerating the body. The middle and hind legs are in advantageous positions to turn the body while minimizing net $\Delta\theta$ from initially positive rotational velocities or when acceleration is advantageous. Whether animals utilize their morphological design to simplify the execution of an array of different maneuvers under different conditions is a behavioral question that deserves future study.

Appendix

The leg effectiveness number that we present depends on the assumptions that the fore–aft axis and the heading remain parallel, and that the movement of the foot relative to the body and heading during a turn is approximately linear (solely in the fore–aft or heading direction). These assumptions are reasonable given the small (approximately 5°) mean difference measured between the fore–aft axis and heading (Table 2) and that the motions of the outside legs are approximately parallel to the fore–aft axis (Fig. 5). Foot positions and forces expressed relative to the heading axis are thus assumed to equal foot positions and forces expressed relative to the fore–aft axis. Movements of the COM and rotation of the body are assumed not to cause the foot position to deviate substantially from a linear trajectory. P_h decreases with constant velocity, and P_p remains approximately constant. Consequently, we would expect ε to describe only turns of relatively small magnitude. Simulations with a less simplified model show that errors in the resulting deflection and rotation from forces calculated using ε are expected to be small for leg position values in the neighborhood of those used by the cockroach and for the mean rotations per step observed in the present study.

Assume that an animal produces constant perpendicular force F_p over a complete step of period τ, during which it moves at a constant velocity V and the trajectory of its foot does not deviate substantially from movement parallel to the heading axis. The movement of the foot parallel to the heading axis over time $P_h(t)$ will be linear, starting from the initial position $P_{AEP,ih}$:

$$P_h(t) = P_{AEP,ih} - Vt \,. \tag{A1}$$

The torque T_p generated by F_p depends on the foot position over time:

$$T_p = F_p P_h(t) \,. \tag{A2}$$

The body rotation, θ_p, resulting from this torque is the torque divided by the moment of inertia, I, twice integrated:

$$\theta_p = \int_{t=0}^{t=\tau}\int_{t=0}^{t=\tau} \frac{T_p}{I}\,dt\,dt = \int_{t=0}^{t=\tau}\int_{t=0}^{t=\tau} \frac{F_p P_h(t)}{I}\,dt\,dt = \int_{t=0}^{t=\tau}\int_{t=0}^{t=\tau} \frac{F_p(P_{AEP,ih} - Vt)}{I}\,dt\,dt \,, \tag{A3}$$

$$\theta_p = \frac{F_p P_{AEP,ih} \tau^2}{2I} - \frac{F_p V \tau^3}{6I} + C\,, \quad \text{(A4)}$$

where C is a constant.

If the animal initially has zero rotational velocity and position, then C=0. In the simple case of an animal turning around a circular trajectory, it will maintain a constant speed V and deflect its COM through an angle θ_d during a period τ. The radius of curvature R is dependent on V, τ and θ_d:

$$R = \frac{V\tau}{\theta_d}\,. \quad \text{(A5)}$$

The animal needs to generate a net perpendicular force F_p to deflect the COM:

$$F_p = \frac{mV^2}{R} = \frac{mV\theta_d}{\tau}\,. \quad \text{(A6)}$$

Given the magnitude of the perpendicular force, we can rewrite equation A4 to express θ_p:

$$\theta_p = \frac{mV\theta_d P_{AEP,ih}\tau^2}{2I\tau} - \frac{mV^2\theta_d\tau^3}{6I\tau} \quad \text{(A7)}$$

or

$$\frac{\theta_p}{\theta_d} = \frac{mV\tau}{2I}\left(P_{AEP,ih} - \frac{V\tau}{3}\right), \quad \text{(A8)}$$

which is the leg effectiveness number ε.

θ_d is the magnitude of the deflection and also the magnitude of the desired rotation. The amount of additional rotation that the force along the heading axis must generate is thus:

$$\theta_d - \theta_p = (1-\varepsilon)\theta_d\,. \quad \text{(A9)}$$

The animal must produce a torque T_h to rotate the body appropriately. T_h is simply the product of the force along the heading axis F_h and the perpendicular position of the foot from the COM, P_p. Since we assume that P_p is constant over the step:

$$(1-\varepsilon)\theta_d = \int_{t=0}^{t=\tau}\int_{t=0}^{t=\tau} \frac{F_h P_p}{I}\,dt\,dt = \frac{F_h P_p \tau^2}{2I} + C\,. \quad \text{(A10)}$$

Or, beginning from initially zero rotational velocity and position and rearranging:

$$F_h P_p = \frac{2(\varepsilon-1)\theta_d I}{\tau^2}\,. \quad \text{(A11)}$$

At a constant mass m and moment of inertia I, given V, τ, θ_d and $P_{AEP,ih}$, ε is also constant and equation A11 can be simplified to:

$$F_h P_p = K\,, \quad \text{(A12)}$$

where K is simply the right-hand side of equation A11. Velocity changes due to F_h are small for relatively small turns and are ignored in this simple model.

The total rotation of the animal will equal the sum of θ_p (equation A4) and the rotation due to F_h. The rotation due to F_h (θ_h) is given by:

$$\theta_h = -\frac{F_h P_p \tau^2}{2I}\,. \quad \text{(A13)}$$

Given equation A7, and assuming the total rotation is θ_d:

$$\theta_d = \theta_p + \theta_h\,, \quad \text{(A14)}$$

$$\theta_d = \frac{mV\theta_d P_{AEP,ih}\tau}{2I} - \frac{mV^2\theta_d\tau^2}{6I} - \frac{F_h P_p \tau^2}{2I}\,. \quad \text{(A15)}$$

Or, holding all variables but F_h and P_h constant:

$$K_1 F_h - K_2 P_{AEP,ih} = 1\,, \quad \text{(A16)}$$

where:

$$K_1 = \frac{P_p\tau^2}{2I\theta_d + (mV^2\theta_d\tau^2)/3}\,, \quad \text{(A17)}$$

$$K_2 = \frac{mV\tau}{2I + (mV^2\tau^2)/3}\,. \quad \text{(A18)}$$

Larger or smaller torque impulses may be necessary to rotate the body if it has an initial rotational velocity. The initial rotational velocity contributes to θ_p:

$$\frac{\theta_p}{\theta_d} = \frac{mV\tau}{2I}\left(P_{AEP,ih} - \frac{V\tau}{3}\right) + \frac{\omega\tau}{\theta_d}\,. \quad \text{(A19)}$$

During steady-speed, straight-ahead running, rotational velocity reaches a minimum at step transitions (Kram et al., 1997), so the assumption of ω=0 at the beginning of a turn is reasonable. During turning, rotational velocity was directed towards the trial turn direction for the majority of steps (Table 2), which would cause the torque impulses due to forces along the heading axis necessary to rotate the body to decrease, thus decreasing the predicted forces along the heading axis required of the legs. However, since the contribution of angular velocity to rotation is likely to be different for the first and subsequent steps, and is unlikely greatly to change the predictions of the model, we considered only the case of initially zero rotational velocity.

List of symbols

a_I–a_{IV}, a_{IV}*	areas of quadrants I–IV (see Fig. 7 in Full et al., 1995)
AEP, PEP	anterior, posterior extreme position
C, K, K_1, K_2	constants
COM	center of mass
F	resultant horizontal force
F_h	component of F in the direction parallel to the heading
F_p	component of F in the direction perpendicular to the heading
I	moment of inertia about the vertical (yaw) axis

l	moment arm
LMN	linear maneuverability number
m	body mass
M_1	slope of the relationship between the quadrant span and σ_h (see Full et al., 1995)
M_2	slope of the relationship between the quadrant ratio and σ_h/σ_t (see Full et al., 1995)
$P_{AEP,ih}$	initial location of the foot in the initial heading direction at the beginning of the step
P_h	location of a foot relative to the center of mass in the direction parallel to the heading
P_p	location of foot relative to the center of mass in the direction perpendicular to the heading
r	distance from the center of mass to a foot
r_{AEP}	distance from the center of mass to a foot at the AEP
r_{PEP}	distance from the center of mass to a foot at the PEP
R	radius of curvature
t	time
V	speed of the center of mass
ε	leg effectiveness number
$\Delta\mathbf{L}$	torque impulse
$\Delta\mathbf{L}_{leg}$	torque impulse generated by an individual leg
$\Delta\mathbf{P}$	force impulse in the direction perpendicular to the initial heading
$\Delta\mathbf{P}_{leg}$	force impulse in the direction perpendicular to the initial heading generated by an individual leg
$\Delta\theta$	degree of misalignment between the fore–aft axis and the heading ($\Delta\theta=\theta_r-\theta_d$)
ϕ	angle between the fore–aft axis and a foot
ϕ_{AEP}	angle between the fore–aft axis and a foot at the AEP
ϕ_{PEP}	angle between the fore–aft axis and a foot at the PEP
θ_d	angular change of heading (magnitude of deflection) relative to the global coordinate frame
θ_r	angular change of the fore–aft axis (magnitude of rotation) relative to the global coordinate frame
θ_p	change in orientation of the fore–aft axis relative to the coordinate frame set by the initial fore–aft axis due to a force perpendicular to the heading
θ_h	change in orientation of the fore–aft axis relative to the coordinate frame set by the initial fore–aft axis due to a force parallel to the heading
σ_h	horizontal stress
σ_t	total stress
τ	step period
T	torque about the center of mass
T_p	torque about the center of mass caused by F_p
T_h	torque about the center of mass caused by F_h
ω	rotational velocity

This work was supported by an NSF Graduate Research Fellowship to D.L.J., ONR Grant N00014-92-J-1250 and DARPA Grant N00014-98-I-0747 to R.J.F. We would like to acknowledge Tim Kubow for his insights and contributions, and James Glasheen for deriving the linear maneuverability number. We would also like to acknowledge Jeremy Berger and John Chung for assisting in data collection and analysis, and Kellar Autumn for statistical advice. We would also like to acknowledge Andre Seyfarth, Rodger Kram and the Berkeley Biomechanics group for critically reading the manuscript.

References

Alexander, R. McN. (1971). *Size and Shape*. London: Edward Arnold.

Alexander, R. McN. (1990). Three uses for springs in legged locomotion. *Int. J. Robotics Res.* **9**, 53–61.

Biewener, A. A. and Full, R. J. (1992). Force platform and kinematic analysis. In *Biomechanics: Structures and Systems, a Practical Approach* (ed. A. A. Biewener), pp. 45–73. Oxford: IRL Press at Oxford University Press.

Blickhan, R. (1989). The spring-mass model for running and hopping. *J. Biomech.* **22**, 1217–1227.

Blickhan, R. and Full, R. J. (1987). Locomotion energetics of the ghost crab. II. Mechanics of the centre of mass during walking and running. *J. Exp. Biol.* **130**, 155–174.

Blickhan, R. and Full, R. J. (1993). Similarity in multilegged locomotion: bouncing like a monopode. *J. Comp. Physiol.* A **173**, 509–517.

Camhi, J. M. and Johnson, E. N. (1999). High-frequency steering maneuvers mediated by tactile cues: antennal wall-following in the cockroach. *J. Exp. Biol.* **202**, 631–643.

Camhi, J. M. and Levy, A. (1988). Organization of a complex movement: fixed and variable components of the cockroach escape behavior. *J. Comp. Physiol.* A **163**, 317–328.

Cavagna, G. A., Heglund, N. C. and Taylor, C. R. (1977). Mechanical work in terrestrial locomotion: two basic mechanisms for minimizing energy expenditure. *Am. J. Physiol.* **233**, R243–R261.

Cruse, H. and Silva Saavedra, M. G. S. (1996). Curve walking in crayfish. *J. Exp. Biol.* **199**, 1477–1482.

Domenici, P., Jamon, M. and Clarac, F. (1998). Curve walking in freely moving crayfish (*Procambarus clarkii*). *J. Exp. Biol.* **201**, 1315–1329.

Farley, C., Glasheen, J. and McMahon, T. A. (1993). Running springs: speed and animal size. *J. Exp. Biol.* **185**, 71–86.

Franklin, R., Bell, W. J. and Jander, R. (1981). Rotational locomotion by the cockroach *Blattella germanica*. *J. Insect Physiol.* **27**, 249–255.

Frantsevich, L. I. and Mokrushov, P. A. (1980). Turning and righting in *Geotrupes* (Coleoptera, Scarabeidae). *J. Comp. Physiol.* **136**, 279–289.

Full, R. J. (1989). Mechanics and energetics of terrestrial locomotion: bipeds to polypeds. In *Energy Transformations in Cells and Organisms. Proceedings of the 10th Conference of the European Society for Comparative Physiology and Biochemistry* (ed. W. Wieser and E. Gnaiger), pp. 175–181. Innsbruck, Stuttgart, New York: Georg Thieme Verlag.

Full, R. J. and Ahn, A. N. (1995). Static forces and moments generated in the insect leg: comparison of a three-dimensional musculoskeletal computer model with experimental measurements. *J. Exp. Biol.* **198**, 1285–1298.

Full, R. J., Blickhan, R. and Ting, L. H. (1991). Leg design in hexpedal runners. *J. Exp. Biol.* **158**, 369–390.

Full, R. J. and Farley, C. T. (1999). Musculoskeletal dynamics in rhythmic systems – a comparative approach to legged locomotion. In *Biomechanics and Neural Control of Movement* (ed. J. M. Winters and P. E. Crago). NewYork: Springer-Verlag (in press).

Full, R. J., Stokes, D. R., Ahn, A. N. and Josephson, R. K. (1998). Energy absorption during running by leg muscles in a cockroach. *J. Exp. Biol.* **201**, 997–1012.

Full, R. J. and Tu, M. S. (1990). Mechanics of six-legged runners. *J. Exp. Biol.* **148**, 129–146.

Full, R. J. and Tu, M. S. (1991). Mechanics of a rapid running insect: two-, four- and six-legged locomotion. *J. Exp. Biol.* **156**, 215–231.

Full, R. J., Yamauchi, A. and Jindrich, D. L. (1995). Maximum single leg force production: cockroaches righting on photoelastic gelatin. *J. Exp. Biol.* **198**, 2441–2452.

Götz, K. G. and Wenking, H. (1973). Visual control of locomotion in the walking fruitfly *Drosophila*. *J. Comp. Physiol.* **85**, 235–266.

Graham, D. (1972). A behavioural analysis of the temporal organisation of walking movements in the 1st instar and adult stick insect (*Carausius morosus*). *J. Comp. Physiol.* **81**, 23–52.

Greene, P. R. (1985). Running on flat turns: experiments, theory and applications. *Biomech. Engng* **107**, 96–103.

Hughes, R. N. (1989). Essential involvement of specific legs in turn alternation of the woodlouse, *Porcellio scaber*. *Comp. Biochem. Physiol.* **93**A, 493–497.

Jamon, M. and Clarac, F. (1995). Locomotion patterns on freely moving crayfish (*Procambarus clarkii*). *J. Exp. Biol.* **198**, 683–700.

Jander, J. P. (1985). Mechanical stability in stick insects when walking straight and around curves. In *Insect Locomotion* (ed. M. Gewecke and G. Wendler), pp. 33–42. Berlin: Paul Parey.

Kram, R., Wong, B. and Full, R. J. (1997). Three-dimensional kinematics and limb kinetic energy of running cockroaches. *J. Exp. Biol.* **200**, 1919–1929.

Land, M. (1972). Stepping patterns made by jumping spiders during turns mediated by the lateral eyes. *J. Exp. Biol.* **56**, 15–40.

McMahon, T. A. and Cheng, G. C. (1990). The mechanics of running: how does stiffness couple with speed? *J. Biomech.* **23**, 65–78.

Pearson, K. G. (1972). Central programming and reflex control of walking in the cockroach. *J. Exp. Biol.* **56**, 173–193.

Schaefer, P. L., Kondagunta, V. and Ritzmann, R. E. (1994). Motion analysis of escape movements evoked by tactile stimulation in the cockroach *Periplaneta americana*. *J. Exp. Biol.* **190**, 287–294.

Siegel, S. (1956). *Nonparametric Statistics for the Behavioral Sciences*. New York: McGraw Hill. 312pp.

Strauß, R. and Heisenberg, M. (1990). Coordination of legs during straight walking and turning in *Drosophila melanogaster*. *J. Comp. Physiol.* A **167**, 403–412.

Tauber, E. and Camhi, J. M. (1995). The wind-evoked escape behavior of the cricket *Gryllus bimaculatus*: integration of behavioral elements. *J. Exp. Biol.* **198**, 1895–1907.

Ting, L. H., Blickhan, R. and Full, R. J. (1994). Dynamic and static stability in hexapedal runners. *J. Exp. Biol.* **197**, 251–269.

Watson, J. T. and Ritzmann, R. E. (1998). Leg kinematics and muscle activity during treadmill running in the cockroach, *Blaberus discoidalis*. I. Slow running. *J. Comp. Physiol.* A **182**, 11–22.

Zollikofer, C. P. (1994). Stepping patterns in ants. I. Influence of speed and curvature. *J. Exp. Biol.* **192**, 95–106.

Zolotov, V., Frantsevich, L. and Falk, E. M. (1975). Kinematik der phototaktischen Drehung bei der Honigbiene *Apis mellifera* L. *J. Comp. Physiol.* **97**, 339–353.